

Self-Calibration Technique for 3-point Intrinsic Alignment Correlations in Weak Lensing Surveys

M. A. Troxel^{*} and M. Ishak^{†1}

¹*Department of Physics, The University of Texas at Dallas, Richardson, TX 75083, USA*

7 January 2021

ABSTRACT

The intrinsic alignment (IA) of galaxies has been shown to be a significant barrier to precision cosmic shear measurements. (Zhang, 2010, ApJ, 720, 1090) proposed a self-calibration technique for the power spectrum to calculate the induced gravitational shear-galaxy intrinsic ellipticity correlation (GI) in weak lensing surveys with photo-z measurements which is expected to reduce the IA contamination by at least a factor of 10 for currently proposed surveys. We confirm this using an independent analysis and propose an expansion to the self-calibration technique for the bispectrum in order to calculate the dominant IA gravitational shear-gravitational shear-intrinsic ellipticity correlation (GGI) contamination. We first establish an estimator to extract the galaxy density-density-intrinsic ellipticity (ggI) correlation from the galaxy ellipticity-density-density measurement for a photo-z galaxy sample. We then develop a relation between the GGI and ggI bispectra, which allows for the estimation and removal of the GGI correlation from the cosmic shear signal. We explore the performance of these two methods, compare to other possible sources of error, and show that the GGI self-calibration technique can potentially reduce the IA contamination by up to a factor of 5-10 for all but a few bin choices, thus reducing the contamination to the percent level. The self-calibration is less accurate for adjacent bins, but still allows for a factor of three reduction in the IA contamination. The self-calibration thus promises to be an efficient technique to isolate both the 2-point and 3-point intrinsic alignment signals from weak lensing measurements.

Key words: gravitational lensing – cosmology

1 INTRODUCTION

Weak gravitational lensing due to large scale structure (cosmic shear) has emerged as a powerful cosmological probe in order to map the distribution of dark matter in the universe and to characterise the equation of state of dark energy, improving constraints on the equation of state of dark energy and the matter fluctuation amplitude parameter by factors of 2 to 4 (see for example Bacon, Refregier & Ellis (2000); Brown et al. (2003); Eisenstein, Hu & Tegmark (1999); Fu, Wu & Yu (2009); Hoekstra et al. (2002); Hu & Tegmark (1999); Hu (2002); Jarvis et al. (2003); Joudaki, Cooray & Holz (2009); Massey et al. (2005); Pen et al. (2003); Rhodes, Refregier & Groth (2001); Schrabback et al. (2010); Van Waerbeke et al. (2000, 2002); Zaldarriaga, Spergel & Seljak (1997) and references therein.) Gravitational lensing has also been shown to be very useful to test the nature of gravity at cosmological distance scales (see for example the partial list Acquaviva et al. (2008); Bean & Tangmatitham (2010); Capozziello, Cardone & Troisi (2006); Daniel et al. (2008, 2010); Dossett, Moldenhauer & Ishak (2011); Huterer & Linder (2007); Ishak, Upadhye & Spergel (2006); Ishak & Dossett (2009); Linder & Cahn (2007); Schmidt (2008); Song (2005); Thomas, Abdalla & Weller (2009); Toreno, Semboloni & Schrabback (2010); Zhang et al. (2007); Zhao et al. (2006, 2009).)

In addition to the constraints obtained from the 2-point cosmic shear correlation and the corresponding shear power

^{*} Electronic address: troxel@utdallas.edu

[†] Electronic address: mishak@utdallas.edu

spectrum, the 3-point cosmic shear correlation and the shear bispectrum have been shown to break degeneracies in the cosmological parameters that the power spectrum alone does not (Takada & Jain 2003; Vafaei et al. 2010). For example, the results of Takada & Jain (2004) showed that a deep lensing survey should be able to improve the constraints on the dark energy parameters and the matter fluctuation amplitude by a further factor of 2-3 using the bispectrum, and most recently, Semboloni et al. (2010) derived parameter constraints by measuring the third order moment of the aperture mass measure using weak lensing data from the HST COSMOS survey. They found independent results consistent with WMAP7 best-fit cosmology, and an improved constraint when combined with the 2-point correlation. Ongoing, future and proposed lensing surveys (e.g. CFHTLS¹, DES², EUCLID³, HSC⁴, HST⁵, JWST⁶, LSST⁷, Pan-STARRS⁸, and WFIRST⁹) promise to provide precision cosmic shear measurements.

Cosmic shear measurements are limited in precision by several systematic effects. It is important to understand and control these systematic effects in order to fully explore the potential of this probe (see for example Bacon et al. (2001); Bernstein & Jarvis (2002); Catelan, Kamionkowski & Blandford (2001); Croft & Metzler (2000); Erben et al. (2001); Heavens, Refregier & Heymans (2000); Heymans et al. (2004); Hirata & Seljak (2003a); Ishak et al. (2004); King & Schneider (2002); Refregier (2003); Takada & White (2004); Van Waerbeke & Mellier (2003); Brown et al. (2002) and references therein). One of the serious systematic effects of lensing is the correlated intrinsic alignment of galaxies which contaminates the lensing signal and acts as a nuisance factor (see for example Brown et al. (2002); Blazek, McQuinn & Seljak (2011); Catelan, Kamionkowski & Blandford (2001); Crittenden et al. (2001); Croft & Metzler (2000); Heymans & Heavens (2003); Hirata & Seljak (2003b); Jing (2002); Krause & Hirata (2011); Bridle & King (2007); Joachimi & Bridle (2010); Hirata et al. (2007); Hirata & Seljak (2004); Mandelbaum et al. (2006); Heymans et al. (2006); Faltenbacher et al. (2009); Okumura T., Jing (2009); Joachimi et al. (2010); Semboloni et al. (2008); King (2005); King & Schneider (2002, 2003); Kirk, Bridle & Schneider (2010) and references therein). For example, Bridle & King (2007); Joachimi & Bridle (2010) showed that if intrinsic alignment is ignored the determination of the dark energy equation of state is biased by as much as 50%. Hirata et al. (2007) found that the matter power spectrum amplitude can be affected by intrinsic alignment by up to 30%, showing the importance of developing methods to isolate the intrinsic alignment and remove it from the cosmic shear signal.

There are two 2-point intrinsic alignment correlations. The first is a correlation between the intrinsic ellipticity of two galaxies, known as the II correlation. If the two galaxies are spatially close, they can be aligned by the tidal force field of the same nearby matter structure. The second intrinsic alignment correlation, known as the GI correlation, was identified by Hirata & Seljak (2004) and is due to a matter structure both causing the alignment of a nearby galaxy and contributing to the lensing signal of a background galaxy. This produces an anti-correlation between the cosmic shear and intrinsic ellipticity, since the tidal force and gravitational lensing tend to align the galaxy shapes in orthogonal directions. The GI correlation has been measured in various subsets of the SDSS spectroscopic and imaging samples by various groups. A detection of the large-scale GI correlation in the SDSS was reported by Mandelbaum et al. (2006) and then Hirata et al. (2007) found an even stronger GI correlation for Luminous Red Galaxies (LRGs). It was shown in these papers that this contamination can affect the lensing measurement and cosmology up to the 10% level and up to 30% in some cases for the matter fluctuation amplitude. This finding was confirmed by numerical simulations, where a level of contamination of 10% was found (Heymans et al. 2006). Further measurements of the GI correlation were made in the SDSS dataset by Faltenbacher et al. (2009); Okumura T., Jing (2009). Most recently, Joachimi et al. (2010) measured strong 2-point intrinsic alignment correlations in various SDSS and MegaZ-LRG samples.

In a similar way, when we consider three galaxies and the related 3-point correlation, the cosmic shear signal (GGG bispectrum) also suffers from contamination by the 3-point intrinsic alignment correlations. The first is the III correlation between intrinsic ellipticities of three spatially close galaxies which are intrinsically aligned by a nearby matter structure. The second is the GII correlation, where two spatially close galaxies are intrinsically aligned by a nearby matter structure which contributes to the lensing of a third galaxy in the background. Finally, there is the GGI correlation, where two galaxies are lensed by a structure which intrinsically aligns a third galaxy in the foreground. Unlike the 2-point correlations, the sign of the GGI and GII correlations depend both on triangle shape and scale. Semboloni et al. (2008) showed that lensing bispectrum measurements are typically more strongly contaminated by intrinsic alignment compared to the lensing spectrum measurements, and that the contamination from the 3-point intrinsic alignment correlation can be as large as 15 – 20%

¹ <http://www.cfht.hawaii.edu/Science/CFHLS/>

² <http://www.darkenergysurvey.org/>

³ <http://sci.esa.int/euclid/>

⁴ <http://www.naoj.org/Projects/HSC/>

⁵ <http://www.stsci.edu/hst/>

⁶ <http://www.jwst.nasa.gov/>

⁷ <http://www.lsst.org/lsst/>

⁸ <http://pan-starrs.ifa.hawaii.edu/>

⁹ <http://wfirst.gsfc.nasa.gov/>

compared to the GGG lensing signal. Finally, 3-point intrinsic alignment measurements are not only useful for constraining their contamination to 3-point lensing measurements, but are also useful for constraining models of intrinsic alignments and therefore constraining the contamination to all lensing measurements (including 2-point correlations) which will dominate the science cases of upcoming surveys.

While the II and III intrinsic alignment correlations can be greatly reduced with photo- z 's by using cross-spectra of galaxies in two different redshift bins (see for example Refregier (2003)) so that the galaxies are separated by large enough distances to assure that the tidal effect is weak, this does not work for the GI, GGI, and GII correlations which happen between galaxies at different redshifts and large separations. The GI correlation and methods for its removal have been the topic of several recent scientific publications and we review these briefly. Initially, some first suggestions were discussed by Hirata & Seljak (2004). King (2005) extended the approach of template fitting by King & Schneider (2002, 2003) to include a treatment of the GI correlation. Bridle & King (2007); Joachimi & Bridle (2010) investigated the effects of the GI correlation on cosmological parameter constraints by assuming a model of the GI intrinsic alignment that is binned in redshift and angular frequency with some free parameters that are marginalised over. Kirk, Bridle & Schneider (2010) performed a cosmological constraint analysis where modelling of intrinsic alignment was included, showing a significant effect on the amplitude of matter fluctuations. Using a geometrical approach, Joachimi & Schneider (2008, 2009, 2010) proposed a nulling technique to remove the GI intrinsic alignment contribution by exploiting the redshift dependence of the correlations, but it is found that the technique throws out some of the valuable lensing signal. Most recently, the nulling technique has been applied at the 3-point level for the GGI correlation, but again with similar signal loss to that at the 2-point level (Shi, Joachimi & Schneider 2010).

Finally, Zhang (2010a) proposed a technique to self-calibrate the GI intrinsic alignment signal by using the intrinsic galaxy ellipticity-galaxy density correlation, which requires that in addition to the galaxy ellipticity-ellipticity correlation (cosmic shear), one should also extract galaxy density-density and galaxy ellipticity-density correlations from the lensing survey. The GI correlation is then calculated and removed from the lensing signal. Most recently, Zhang (2010b) showed that redshift dependencies of intrinsic alignment can allow further improvements to the calculation of the intrinsic alignment contamination. The technique is commonly referred to as self-calibration because it uses correlations that can be extracted from the same gravitational lensing survey and used in order to calculate the GI contamination to the cosmic shear signal and remove it. Joachimi & Bridle (2010) applied an approach like the self-calibration, using correlations between lensing, intrinsic alignment, number density and magnification effects to constrain cosmological parameters. They found that the extra information from the additional correlations can make up for the additional free parameters in the intrinsic alignment so that the contamination can be removed without loss of constraining power.

We organize the paper as follows. In Sec. 2, we briefly discuss the necessary survey parameters and lensing formalism. We then provide a summary of the 2-point GI self-calibration technique of Zhang with independent results. In Sec. 3, we develop the 3-point GGI self-calibration. We first establish an estimator to extract the galaxy density-density-intrinsic ellipticity correlation (ggI) from the observed galaxy ellipticity-density-density measurement for a photo- z galaxy sample. We then develop a relation between the GGI and ggI bispectra, which allows for the estimation and removal of the GGI intrinsic alignment correlation from the cosmic shear signal. Section 4 describes the residual sources of error to the GGI self-calibration technique, and we present the necessary relations to quantify these errors. These are compared to other sources of error in the bispectrum. Finally, we summarise the effectiveness and impact of the GGI self-calibration in Sec. 5. In the Appendix we expand upon the detailed calculation of the coefficients in the error calculation found in Sec. 4.1 and provide a list of typical expected values.

2 BACKGROUND

2.1 Survey information and weak lensing

As mentioned in the previous section, the self-calibration technique proposed by Zhang (2010a) makes use of the information already found in a lensing survey (Bernstein 2009), including galaxy shape, angular position and photometric redshift, in order to calculate and remove the dominant intrinsic alignment contamination. In our performance calculations, we consider survey parameters to match a survey similar to those of the LSST lensing survey (LSST Science Collaborations and LSST Project 2009), but this is just an example. The GGI self-calibration technique is survey independent and can be applied to reduce the intrinsic alignment contamination in all lensing surveys. Galaxies are assumed to be sufficiently large and bright to be suitable for cosmic shear measurements, so we restrict any discussion of the self-calibration to these galaxies in order to avoid any sample bias. Galaxies are split into photo- z bins according to photo- z z^P , where the i -th photo- z bin is described by a mean photo- z \bar{z}_i and has a range $\bar{z}_i - \Delta z_i/2 \leq z^P \leq \bar{z}_i + \Delta z_i/2$. In our notation, $i < j$ implies that $\bar{z}_i < \bar{z}_j$. The galaxy redshift distribution over the i -th redshift bin is $n_i^P(z^P)$ and $n_i(z)$ as a function of photo- z and true redshift, respectively, which are related by the photo- z probability distribution function $p(z|z^P)$.

In evaluating the performance of the self-calibration technique, we will consider as an example survey parameters to match

an LSST-like weak lensing survey (LSST Science Collaborations and LSST Project 2009), but of course the calculations are applicable to all current and planned weak lensing surveys (e.g. CFHTLS, DES, EUCLID, HSC, HST, JWST, LSST, Pan-STARRS, and WFIRST). We assume a survey coverage of half the sky ($f_{sky} = 0.5$) with a total galaxy surface density of 40 arcminute⁻² and redshift density distribution of

$$n(z) = \frac{1}{2z_0} \left(\frac{z}{z_0} \right)^2 \exp(-z/z_0), \quad (1)$$

with $z_0 = 0.5$. The ellipticity shape noise is described by $\gamma_{rms} = 0.18 + 0.042z$ and photo-z error by a Gaussian probability distribution function (PDF)

$$p(z|z^P) = \frac{1}{\sqrt{2\pi\sigma_z^2}} \exp\left(-\frac{(z-z^P)^2}{2\sigma_z^2}\right), \quad (2)$$

with $\sigma_z = 0.05(1+z)$. We define photometric redshift bins of width $\Delta z = 0.2$, centred at $\bar{z}_i = 0.2(i+1)$ ($i = 1, \dots, 9$). We do not include redshifts below $z^P = 0.3$, not because of poor performance in the self-calibration, but rather due to the weaker lensing signal at lower redshifts. This artificially increases the fractional errors we evaluate in Sec. 4 with respect to the GGG lensing signal, as is evident in the increasing errors at low redshift in Fig. 3, and is not useful in evaluating the true performance of the self-calibration.

The self-calibration technique relies upon two basic observables from a weak lensing survey. The first is the galaxy surface density of a photo-z bin, δ^Σ , which is a function of the 3D galaxy distribution δ_g . The second necessary observable is the galaxy shape, expressed in terms of ellipticity, which measures the cosmic shear γ . However, this cosmic shear signal is heavily contaminated by the intrinsic ellipticities of galaxies. There is a random component to this intrinsic ellipticity, which is simple to correct and which we ignore in the self-calibration calculations except as part of the shot noise in the error estimations of Sec. 4. A second component of the intrinsic ellipticity is due to the intrinsic alignment of galaxies caused by the gravitational tidal forces of large scale structure and was introduced in Sec. 1.

We will label the measured shear as $\gamma^s = \gamma + \gamma^I$, where γ^I denotes the correlated part of this intrinsic ellipticity due to the intrinsic alignment of galaxies. Since we are concerned only with the weak limit, we will work with the lensing convergence κ instead. Thus from the measured γ^s , we obtain $\kappa^s = \kappa + \kappa^I$. κ is the projected matter over-density along the line of sight. For a flat universe in the Born approximation, the convergence κ of a source galaxy at redshift z_G and direction $\hat{\theta}$ is

$$\kappa(\hat{\theta}) = \int_0^{\chi_G} \delta(\chi_L, \hat{\theta}) W_L(\chi_L, \chi_G) d\chi_L. \quad (3)$$

$W_L(\chi_L, \chi_G)$ is the lensing kernel and $\delta(\chi_L, \hat{\theta})$ is the matter over-density in direction $\hat{\theta}$ and at comoving distance $\chi_L \equiv \chi_L(z_L)$. $\chi_G \equiv \chi_G(z_G)$ is the comoving distance to the source. The comoving distance χ is in units of c/H_0 , where H_0 is the current day Hubble constant. We assume a flat Λ CDM cosmology with $\Omega_m = 0.27$ and $\Omega_\Lambda = 0.73$. The lensing kernel is then

$$W_L(\chi_L, \chi_G) = \frac{3}{2} \Omega_m (1+z_L) \chi_L \left(1 - \frac{\chi_L}{\chi_G}\right) \quad (4)$$

when $z_L < z_G$ and zero otherwise.

In our calculations, we will work in Fourier (multipole ℓ) space with the corresponding spectra to the correlations which can be built from these survey observables. The two-point correlation function is then related to the angular power spectrum and the 3-point correlation function to the angular bispectrum by

$$\begin{aligned} \langle \tilde{\kappa}(\ell_1) \tilde{\kappa}(\ell_2) \rangle &= (2\pi)^2 \delta^D(\ell_1 + \ell_2) C(\ell_1) \\ \langle \tilde{\kappa}(\ell_1) \tilde{\kappa}(\ell_2) \tilde{\kappa}(\ell_3) \rangle &= (2\pi)^2 \delta^D(\ell_1 + \ell_2 + \ell_3) B(\ell_1, \ell_2, \ell_3), \end{aligned} \quad (5)$$

where $\langle \dots \rangle$ denotes the ensemble average and $\delta^D(\ell)$ is the Dirac delta function. For the bispectrum, $\delta^D(\ell_1 + \ell_2 + \ell_3)$ enforces the condition that the three vectors form a triangle in Fourier space. The 2D angular cross-correlation power spectrum is related to the 3D power spectrum and the 2D angular cross-correlation bispectrum to the 3D bispectrum through the Limber approximation

$$\begin{aligned} C_{ij}(\ell) &= \int_0^x \frac{W_i(\chi') W_j(\chi')}{\chi'^2} P(\ell; \chi') d\chi' \\ B_{ijk}(\ell_1, \ell_2, \ell_3) &= \int_0^x \frac{W_i(\chi') W_j(\chi') W_k(\chi')}{\chi'^4} B(\ell_1, \ell_2, \ell_3; \chi') d\chi', \end{aligned} \quad (6)$$

where i, j, k denote the redshift bin and $W_i(\chi)$ are weighting functions which depend on the quantity being correlated. For

example, when correlating weak lensing this is the weighted lensing kernel $W_i(\chi) = \int_0^\chi W_L(\chi', \chi) f_i(\chi') d\chi'$ where $f_i(\chi)$ is the comoving galaxy distribution in the i -th redshift bin.

2.2 The 2-point GI self-calibration

For the power spectrum, Zhang (2010a) proposed the GI self-calibration technique to calculate and remove the GI correlation, quantified by $f^I \equiv C^{IG}/C^{GG}$, from the angular cross-correlation power spectrum between galaxy ellipticity (κ^s) in the i -th and j -th redshift bins. We confirm and summarise the important components of this technique here, as it is a necessary component in our own development of the 3-point GGI self-calibration. We also present independent performance estimates calculated using the linear alignment model for intrinsic alignment of Hirata & Seljak (2004) for the intrinsic alignment as described in Sec. 4.

The following three observable correlations in a lensing survey between galaxy surface density and convergence for $i < j$ are necessary to the GI self-calibration technique:

$$\begin{aligned} C_{ij}^{(1)}(\ell) &\approx C_{ij}^{GG}(\ell) + C_{ij}^{IG}(\ell), \\ C_{ii}^{(2)}(\ell) &= C_{ii}^{gG}(\ell) + C_{ii}^{gI}(\ell), \\ C_{ii}^{(3)}(\ell) &= C_{ii}^{gg}(\ell). \end{aligned} \quad (7)$$

$C_{ij}^{\alpha\beta}$ is the angular cross-correlation power spectrum between quantity α in the i -th redshift bin and β in the j -th redshift bin. $\alpha, \beta \in G, I, g$, where G indicates gravitational lensing (κ), I the correlated galaxy intrinsic alignment (κ^I) and g the galaxy number density distribution (δ^Σ) in the corresponding redshift bin. Thus we denote the GI power spectrum C_{ij}^{IG} in order to preserve the association of each quantity G or I to its redshift bin. By requiring $i < j$ with sufficient photo- z accuracy, C_{ij}^{GI} and C_{ij}^{II} provide negligible contribution to the lensing signal and are neglected in $C_{ij}^{(1)}$. From these observables, $C_{ij}^{IG}(\ell)$ is expressed by using a deterministic galaxy bias $b_1^i(\ell)$ (see Appendix A of Zhang (2010a)) through the scaling relation

$$C_{ij}^{IG}(\ell) \approx \frac{W_{ij}}{b_1^i(\ell)\Pi_{ii}} C_{ii}^{Ig}(\ell), \quad (8)$$

where $W_{ij} \equiv \int_0^\infty d\chi_L \int_0^\infty d\chi_G [W_L(\chi_L, \chi_G) f_i(\chi_L) f_j(\chi_G)]$ and $\Pi_{ii} = \int_0^\infty f_i^2(\chi) d\chi$. $f_i(\chi) = n_i(z) dz/d\chi$ is the true comoving distance distribution of galaxies in the i -th redshift bin and $W_L(\chi_L, \chi_G)$ is the lensing kernel. Using the effects of lensing geometry, $C_{ii}^{Ig}(\ell)$ is isolated from the second observable $C_{ii}^{(2)}(\ell)$ (see Appendix B of Zhang (2010a)) using the estimator

$$\hat{C}_{ii}^{Ig}(\ell) = \frac{C_{ii}^{(2)}|_S(\ell) - Q_2(\ell)C_{ii}^{(2)}(\ell)}{1 - Q_2(\ell)}, \quad (9)$$

with $Q_2(\ell) \equiv C_{ii}^{gG}|_S(\ell)/C_{ii}^{gG}(\ell)$. The subscript S denotes the correlation between only those pairs with $z_G^P < z_i^P$. $Q_2(\ell)$ then measures the relative suppression of the gG signal due to the orientation dependence of the lensing geometry, where $C_{ii}^{gG}|_S(\ell) \ll C_{ii}^{gG}(\ell)$. For spectroscopic (true) redshifts, $C_{ii}^{gG}|_S(\ell) = 0$ and the estimator $\hat{C}_{ii}^{Ig}(\ell)$ is simply $C_{ii}^{Ig}|_S(\ell) = C_{ii}^{gI}(\ell)$, since the gI correlation is independent of orientation. The measurement error (see Appendix C of Zhang (2010a)) in this estimator is

$$\begin{aligned} \Delta C_{ii}^{Ig} &= \frac{1}{2\ell\Delta\ell f_{sky}} \left\{ C_{ii}^{gg} C_{ii}^{GG} + \left(1 + \frac{1}{3(1-Q_2)^2}\right) [C_{ii}^{gg} C_{ii}^{gg,N} + C_{ii}^{gg,N} (C_{ii}^{GG} + C_{ii}^{II})] \right. \\ &\quad \left. + \left(1 + \frac{1}{(1-Q_2)^2}\right) C_{ii}^{gg,N} C_{ii}^{GG,N} \right\}. \end{aligned} \quad (10)$$

The fractional error on C_{ij}^{IG} (and thus the residual statistical error in the measurement of C_{ij}^{GG}) due to ΔC_{ii}^{Ig} is

$$\Delta f_{ij} = \left(\frac{W_{ij}}{b_1^i(\ell)\Pi_{ii}} \right) \frac{\Delta C_{ii}^{Ig}}{C_{ij}^{GG}}. \quad (11)$$

This is also the threshold contamination $f_{ij}^I = f_{ij}^{thresh}$ at which the GI self-calibration will function at S/N=1. Similarly, the scaling relation in Eq. 8 is not exact, and its accuracy is quantified by

$$\epsilon_{ij}^{sys} = \frac{b_1^i(\ell)\Pi_{ii}}{W_{ij}} \frac{C_{ij}^{IG}(\ell)}{C_{ij}^{Ig}(\ell)} - 1. \quad (12)$$

This introduces a residual systematic error in the measurement of C_{ij}^{GG} of $\delta f_{ij} = \epsilon_{ij}^{sys} f_{ij}^I$.

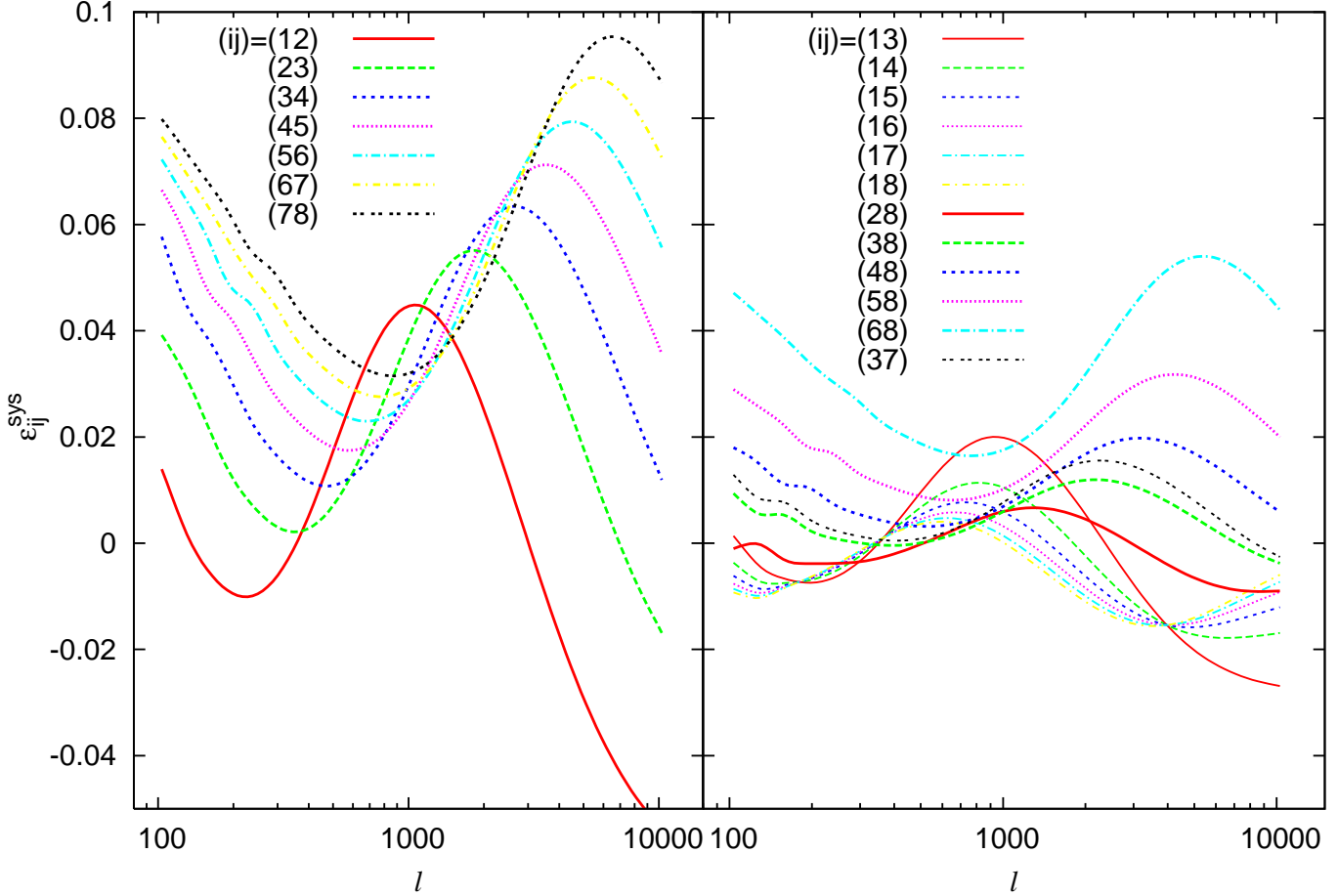


Figure 1. The inaccuracy of the scaling relationship in Eq. 8 is quantified in Eq. 12 by ϵ_{ij}^{sys} . This inaccuracy is the source of the dominant systematic error in the measurement of C_{ij}^{GG} due to the GI self-calibration technique. Left: ϵ_{ij}^{sys} is plotted for adjacent redshift bins, where the stronger dependence of the lensing kernel on redshift causes a significantly higher inaccuracy. Right: ϵ_{ij}^{sys} is plotted for redshift bins of varying distance from each other. As expected, the inaccuracy for these bin choices is generally less than for three adjacent bin choices. Using the linear alignment model for intrinsic alignment of Hirata & Seljak (2004), we find that our result is consistent with the toy model of Zhang (2010a) which gives the smallest systematic error. We thus expect a suppression of the GI intrinsic alignment contamination by at least a factor of 10 for adjacent bins and up to a factor of 50 for other bin pairs. These results are insensitive to the original GI contamination, such that for any $f_{ij}^{tresh} < f_{ij}^I < 1$, the GI self-calibration will reduce the GI contamination down to survey limits or by a factor of 10 or greater, whichever is less.

The third observable $C_{ii}^{(3)}(\ell)$ can be used to calculate the galaxy bias. This gives a result for $C_{ij}^{IG}(\ell)$, which can then be removed from the first observable $C_{ij}^{(1)}(\ell)$. Our notation above, which we will use throughout this paper, is slightly different from the original notation of Zhang (2010a) in order to be compatible with the GGI self-calibration. We denote analogous quantities in the 2- and 3-point self-calibration by the same variable, differentiated by the number of its indices.

The GI self-calibration technique converts a systematic intrinsic alignment contamination f_{ij}^I into a residual statistical error $\Delta f_{ij} < f_{ij}^I$ which is insensitive to the intrinsic alignment contamination. We find good agreement with Zhang’s estimation of the performance of the GI self-calibration, based on independent calculations of the 2-point errors following the methods described in Sec. 4. Figure 1 shows the residual systematic (δf_{ij}) error in the measurement of C_{ij}^{GG} with the GI self-calibration technique. We use the linear alignment model for intrinsic alignment of Hirata & Seljak (2004) and find that our result is consistent with the toy model of Zhang (2010a) which gives the smallest systematic error. We thus expect for an LSST-like lensing survey a suppression of the GI intrinsic alignment contamination by at least a factor of 10 for adjacent bins and up to a factor of 50 for other bin pairs. These results are insensitive to the original GI contamination, such that for any $f_{ij}^{tresh} < f_{ij}^I < 1$, the GI self-calibration will reduce the GI contamination down to survey limits or by a factor of 10 or greater, whichever is less.

3 3-POINT GGI SELF-CALIBRATION

There are several sets of correlations between the observed galaxy surface density and convergence which can be constructed for galaxy triplets. Only three of these observed correlations are needed for the GGI self-calibration technique. The first is the angular cross-correlation bispectrum between galaxy ellipticity (κ^s) in the i -th, j -th and k -th redshift bin

$$B_{ijk}^{(1)}(\ell_1, \ell_2, \ell_3) = B_{ijk}^{GGG}(\ell_1, \ell_2, \ell_3) + B_{ijk}^{IGG}(\ell_1, \ell_2, \ell_3) + (2 \text{ perm.}) + B_{ijk}^{IIG}(\ell_1, \ell_2, \ell_3) + (2 \text{ perm.}) + B_{ijk}^{III}(\ell_1, \ell_2, \ell_3). \quad (13)$$

$B_{ijk}^{\alpha\beta\gamma}$ is the angular cross-correlation bispectrum between quantity α in the i -th redshift bin, β in the j -th redshift bin and γ in the k -th redshift bin. $\alpha, \beta, \gamma \in G, I, g$, where G indicates gravitational lensing (κ), I the correlated galaxy intrinsic alignment (κ^I) and g the galaxy number density distribution (δ^Σ) in the corresponding redshift bin. Unless catastrophic photo- z errors overwhelm the data, we can safely neglect the correlations GII and III which require spatially close galaxies by selecting galaxy triplets where $i < j < k$. Under this requirement, we also have $B_{ijk}^{IGG} \gg B_{ijk}^{GGI}, B_{ijk}^{GIG}$ due to the lensing geometry. We then have for $i < j < k$,

$$B_{ijk}^{(1)}(\ell_1, \ell_2, \ell_3) \approx B_{ijk}^{GGG}(\ell_1, \ell_2, \ell_3) + B_{ijk}^{IGG}(\ell_1, \ell_2, \ell_3). \quad (14)$$

Thus the dominant intrinsic alignment contamination is from the GGI bispectrum $B_{ijk}^{IGG}(\ell_1, \ell_2, \ell_3)$ ($i < j < k$), which the GGI self-calibration technique seeks to calculate and remove. Here we denote the GGI bispectrum B_{ijk}^{IGG} in order to preserve the association of each quantity G or I to its redshift bin, as for the 2-point GI power spectrum.

The second correlation is measured in the angular cross-correlation bispectrum between convergence (κ^s) in the i -th redshift bin and galaxy density (δ^Σ) in the j -th and k -th redshift bins. Of interest to the self-calibration is the case where $i = j = k$, and we have

$$B_{iii}^{(2)}(\ell_1, \ell_2, \ell_3) = B_{iii}^{Ggg}(\ell_1, \ell_2, \ell_3) + B_{iii}^{Igg}(\ell_1, \ell_2, \ell_3). \quad (15)$$

This correlation contributes further information about the intrinsic alignment of galaxies

The final correlation of interest is measured in the angular cross-correlation bispectrum between galaxy density (δ^Σ) in the i -th, j -th and k -th redshift bins when $i = j = k$, giving

$$B_{iii}^{(3)}(\ell_1, \ell_2, \ell_3) = B_{iii}^{ggg}(\ell_1, \ell_2, \ell_3). \quad (16)$$

We also require for the GGI self-calibration those observables in Eq. 7 for the GI self-calibration. It is important to note that we have thus far neglected the contribution of magnification bias to these measurements. This will be further discussed and justified for the 3-point measurements in Sec. 4.3 and was discussed and shown to be negligible for the GI self-calibration by Zhang (2010a). There is also a non-Gaussian contribution to the observed bispectra. We briefly discuss the impact of this non-Gaussianity on the self-calibration technique in Sec. 4.4, but otherwise leave discussion and calculation of this non-Gaussian contribution to the bispectrum to other works.

Our GGI self-calibration technique will calculate and remove the GGI contamination in Eq. 14 by using the measurements from Eqs. 15 & 16, which are both available in the same lensing survey. We express the fractional contamination to the lensing signal by the correlated intrinsic alignment as

$$f_{ijk}^I(\ell_1, \ell_2, \ell_3) \equiv \frac{B_{ijk}^{IGG}(\ell_1, \ell_2, \ell_3)}{B_{ijk}^{GGG}(\ell_1, \ell_2, \ell_3)}. \quad (17)$$

For the self-calibration to work, the contamination $f_{ijk}^I(\ell_1, \ell_2, \ell_3)$ must be sufficiently large as to contribute a detectable $B_{iii}^{Igg}(\ell_1, \ell_2, \ell_3)$ at the corresponding ℓ bins in $B_{iii}^{(2)}(\ell_1, \ell_2, \ell_3)$. We denote this threshold f_{ijk}^{thresh} . When $f_{ijk}^I \geq f_{ijk}^{thresh}$, the GGI self-calibration can be applied to reduce the GGI contamination. The residual error after the GGI self-calibration will be expressed as a residual fractional error on the lensing measurement. In our notation, we differentiate Δf_{ijk} as statistical error and δf_{ijk} as systematic error. The performance of the GGI self-calibration will then be quantified by the parameters f_{ijk}^{thresh} , Δf_{ijk} and δf_{ijk} , which are discussed and calculated in Sec. 4.

3.1 Relationship between B_{ijk}^{IGG} and B_{iii}^{Igg}

The first step in the GGI self-calibration is to determine the relationship between B_{ijk}^{IGG} and B_{iii}^{Igg} . Under the Limber approximation, the 2D GGI angular cross-correlation bispectrum between the i -th, j -th and k -th redshift bins is related to the 3D matter-matter-galaxy intrinsic alignment bispectrum by

$$B_{ijk}^{IGG}(\ell_1, \ell_2, \ell_3) = \int_0^\infty \frac{f_i(\chi)W_j(\chi)W_k(\chi)}{\chi^4} B_{\delta\delta\gamma I} \left(k_1 = \frac{\ell_1}{\chi}, k_2 = \frac{\ell_2}{\chi}, k_3 = \frac{\ell_3}{\chi}; \chi \right) d\chi, \quad (18)$$

where

$$W_i(\chi_L) = \int_0^\infty W_L(\chi_L, \chi_G) f_i(\chi_G) d\chi_G. \quad (19)$$

The integral runs from zero to ∞ in order to take into account the photo-z error. We again denote the GGI bispectrum B_{ijk}^{IGG} in order to preserve the association of each quantity G or I to its redshift bin and will continue this convention throughout the paper. Similarly, the 2D ggI angular auto-correlation bispectrum is related to the 3D galaxy-galaxy-galaxy intrinsic alignment bispectrum by

$$B_{iii}^{Igg}(\ell_1, \ell_2, \ell_3) = \int_0^\infty \frac{f_i^3(\chi)}{\chi^4} B_{gg\gamma I} \left(k_1 = \frac{\ell_1}{\chi}, k_2 = \frac{\ell_2}{\chi}, k_3 = \frac{\ell_3}{\chi}; \chi \right) d\chi. \quad (20)$$

We will adopt a deterministic galaxy bias $b_{g,k}$ (Fry & Gaztanaga 1993) such that the smoothed galaxy density is a function of matter density expressed as

$$\delta_g(\mathbf{x}; \chi) = b_{g,1}(\chi)\delta_m(\mathbf{x}; \chi) + \frac{b_{g,2}(\chi)}{2}\delta_m^2(\mathbf{x}; \chi) + O(\delta^3). \quad (21)$$

The first term $b_{g,1}$ is the linear galaxy bias (as used by Zhang (2010a) for the 2-point correlations). The second term represents the first order non-linear contribution. $b_{g,2}$ is typically found to be negative and $\leq b_{g,1}$ (Cooray & Sheth 2002). Unlike in the 2-point case, it is insufficient to model the bias as simply scale dependent (Jeong & Komatsu 2009). Following the galaxy-galaxy-galaxy halo bispectrum derivation of Jeong & Komatsu (2009), we use this expression of the galaxy density to relate $B_{\delta\delta\gamma I}^{IGG}$ to $B_{gg\gamma I}^{Igg}$. We neglect the portion of the bispectrum due to primordial non-Gaussianity and the trispectrum term, which contains further information about the non-Gaussianity. This is justified and discussed further in Sec. 4.4. This results in the relationship

$$B_{gg\gamma I}(k_1, k_2, k_3; \chi) = b_{g,1}^2(\chi)B_{\delta\delta\gamma I}(k_1, k_2, k_3; \chi) + b_{g,1}(\chi)b_{g,2}(\chi) [P_{\delta\gamma I}(k_1; \chi)P_{\delta\delta}(k_2; \chi) + P_{\delta\delta}(k_2; \chi)P_{\delta\gamma I}(k_3; \chi) + P_{\delta\gamma I}(k_1; \chi)P_{\delta\gamma I}(k_3; \chi)]. \quad (22)$$

If the galaxy bias changes slowly over the i -th redshift bin with median comoving distance χ_i , we can write to a good approximation $b_k^i = b_{g,k}(\chi_i)$. Substituting Eq. 22 into Eq. 20, we have

$$B_{iii}^{Igg}(\ell_1, \ell_2, \ell_3) = \int_0^\infty \frac{f_i^3(\chi)}{\chi^4} \left((b_1^i)^2 B_{\delta\delta\gamma I}(k_1, k_2, k_3; \chi) + b_1^i b_2^i [P_{\delta\gamma I}(k_1; \chi)P_{\delta\delta}(k_2; \chi) + P_{\delta\delta}(k_2; \chi)P_{\delta\gamma I}(k_3; \chi) + P_{\delta\gamma I}(k_1; \chi)P_{\delta\gamma I}(k_3; \chi)] \right) d\chi. \quad (23)$$

We can further approximate $B(k_1, k_2, k_3; \chi) \approx B(k_1, k_2, k_3; \chi_i)$ and $P(k; \chi) \approx P(k; \chi_i)$ in the limit where the comoving distance distribution of galaxies in the i -th redshift bin is narrow. This leads to the following approximations of Eqs. 18 & 23,

$$B_{ijk}^{IGG}(\ell_1, \ell_2, \ell_3) \approx B_{\delta\delta\gamma I}(k_1, k_2, k_3; \chi_i) \frac{W_{ijk}}{\chi_i^4}, \quad (24)$$

and

$$B_{iii}^{Igg}(\ell_1, \ell_2, \ell_3) \approx \frac{\Pi_{iii}}{\chi_i^4} \left((b_1^i)^2 B_{\delta\delta\gamma I}(k_1, k_2, k_3; \chi_i) + b_1^i b_2^i [P_{\delta\gamma I}(k_1; \chi_i)P_{\delta\delta}(k_2; \chi_i) + P_{\delta\delta}(k_2; \chi_i)P_{\delta\gamma I}(k_3; \chi_i) + P_{\delta\gamma I}(k_1; \chi_i)P_{\delta\gamma I}(k_3; \chi_i)] \right), \quad (25)$$

where $W_{ijk} = \int_0^\infty f_i(\chi)W_j(\chi)W_k(\chi)d\chi$ and $\Pi_{iii} = \int_0^\infty f_i^3(\chi)d\chi$. From Eqs. 24 & 25, we have

$$B_{ijk}^{IGG}(\ell_1, \ell_2, \ell_3) \approx \frac{W_{ijk}}{(b_1^i)^2 \Pi_{iii}} B_{iii}^{Igg}(\ell_1, \ell_2, \ell_3) - \frac{b_2^i W_{ijk}}{b_1^i \chi_i^4} \times [P_{\delta\gamma I}(k_1; \chi_i)P_{\delta\delta}(k_2; \chi_i) + P_{\delta\delta}(k_2; \chi_i)P_{\delta\gamma I}(k_3; \chi_i) + P_{\delta\gamma I}(k_1; \chi_i)P_{\delta\gamma I}(k_3; \chi_i)]. \quad (26)$$

In order to express the 3D power spectra in Eq. 26 as 2D spectra, we will use the approximation made by Zhang $C_{ii}^{Ig}(\ell) \approx P_{\delta\gamma I}(k; \chi_i) \frac{b_1^i \Pi_{ii}}{\chi_i^2}$ and the similar approximation $C_{ii}^{GG}(\ell) \approx P_{\delta\delta}(k; \chi_i) \frac{\omega_{ii}}{\chi_i^2}$, where $\omega_{ii} = \int_0^\infty W_i^2(\chi)d\chi$. Equation 26 is then

$$B_{ijk}^{IGG}(\ell_1, \ell_2, \ell_3) \approx \frac{W_{ijk}}{(b_1^i)^2 \Pi_{iii}} B_{iii}^{Igg}(\ell_1, \ell_2, \ell_3) - \frac{b_2^i}{(b_1^i)^2} \frac{W_{ijk}}{\omega_{ii} \Pi_{ii}} \times \left[C_{ii}^{Ig}(\ell_1) C_{ii}^{GG}(\ell_2) + C_{ii}^{GG}(\ell_2) C_{ii}^{Ig}(\ell_3) + \frac{\omega_{ii}}{b_1^i \Pi_{ii}} C_{ii}^{Ig}(\ell_1) C_{ii}^{Ig}(\ell_3) \right]. \quad (27)$$

This relationship, while developed in the same way as for the GI self-calibration, is necessarily more complicated due to the inclusion of the non-linear galaxy bias and the presence of the GG correlation. Thus in order to apply this relationship, it is necessary to not only develop an estimator for $B_{iii}^{Igg}(\ell_1, \ell_2, \ell_3)$, which we describe in Sec. 3.2, but also to use the estimator $\hat{C}_{ii}^{Ig}(\ell)$ in Eq. 9 developed for the GI self-calibration and the resulting $C_{ii}^{GG}(\ell)$, as measured by the GI self-calibration (Zhang 2010a). The GGI self-calibration technique is thus dependent upon the resulting measurements of the GI self-calibration technique.

3.2 B_{iii}^{Igg} Measurement

Information about the galaxy density-density-intrinsic ellipticity bispectrum, B_{iii}^{Igg} , is contained within the observable $B_{iii}^{(2)} = B_{iii}^{Igg} + B_{iii}^{Ggg}$. To measure it directly, we must first remove the contamination of B_{iii}^{Ggg} . For a spectroscopic galaxy sample, lensing geometry requires eliminating those triplets of galaxies where the redshift of the galaxy used to measure the ellipticity is lower than those used to measure galaxy number density. In this way, those triplets remaining have no contamination from B_{iii}^{Ggg} and measure only B_{iii}^{Igg} .

In the case of a photo-z galaxy sample, this is not possible due to typically large photo-z error. Even for a photo-z bin with $\Delta z \rightarrow 0$, the photo-z error causes a true redshift distribution of width $\geq 2\sigma_P = 0.1(1+z)$. In practice, photo-z bins are typically ≥ 0.2 . With such large errors, it is possible for galaxy triplets in the i -th redshift bin to provide a measureable lensing contribution to B_{iii}^{Ggg} even when requiring that the redshift of the galaxy used to measure the ellipticity is lower than those used to measure galaxy number density, except for the special cases where we limit to sufficiently low values the redshift or both the photo-z error and bin size. A more careful approach is thus required when separating B_{iii}^{Igg} from B_{iii}^{Ggg} for a general photo-z galaxy sample.

We apply the approach used by Zhang for the power spectrum $C_{ii}^{(2)}$ to the bispectrum $B_{iii}^{(2)}$, wherein we consider the orientation dependence of the two components. We will first define a redshift for each galaxy in the triplet: $z_{G/I}$ for the galaxy used in the lensing/intrinsic alignment measurement and $z_g, z_{g'}$ for the two galaxies used in the number density measurement. The ggI correlation is independent of the relative position of the three galaxies. For example, the correlations with $z_I < z_g < z_{g'}$, $z_g < z_I < z_{g'}$ or $z_g < z_{g'} < z_I$ are statistically identical when the sides of the triangle are fixed. However, the Ggg correlation does depend on the relative position of the three galaxies. Due to the lensing geometry dependence, the correlation with $z_G < z_g, z_{g'}$ is statistically smaller than other orientations.

This dependence provides two observables from $B_{iii}^{(2)}$. The first is $B_{iii}^{(2)}$, where all triplets are weighted equally. The second is $B_{iii}^{(2)}|_S$, which counts only those triplets with $z_G < z_g, z_{g'}$. This weighting is denoted by the subscript 'S'. From our previous discussion, we then have $B_{iii}^{Igg} = B_{iii}^{Igg}|_S$ and $B_{iii}^{Ggg} > B_{iii}^{Ggg}|_S$. We now define the ratio

$$Q_3(\ell_1, \ell_2, \ell_3) \equiv \frac{B_{iii}^{Ggg}|_S(\ell_1, \ell_2, \ell_3)}{B_{iii}^{Ggg}(\ell_1, \ell_2, \ell_3)}, \quad (28)$$

where we have explicitly included the ℓ -dependence which had been neglected previously in this section. This ratio describes the suppression of the signal due to the weighting of triplets described previously. By definition $0 < Q_3 < 1$, with $Q_3 = 0$ if the photo-z is perfectly accurate and $Q_3 = 1$ if the photo-z has no correlation to the true redshift. Q_3 is calculated using the galaxy redshift distribution, which is discussed in Sec. 3.3.

We now define an estimator for B_{iii}^{Igg} (that we denote \hat{B}_{iii}^{Igg}) in terms of $Q_3(\ell_1, \ell_2, \ell_3)$ and the two observables

$$\begin{aligned} B_{iii}^{(2)}(\ell_1, \ell_2, \ell_3) &= B_{iii}^{Igg}(\ell_1, \ell_2, \ell_3) + B_{iii}^{Ggg}(\ell_1, \ell_2, \ell_3), \\ B_{iii}^{(2)}|_S(\ell_1, \ell_2, \ell_3) &= B_{iii}^{Igg}|_S(\ell_1, \ell_2, \ell_3) + B_{iii}^{Ggg}|_S(\ell_1, \ell_2, \ell_3). \end{aligned} \quad (29)$$

This estimator is

$$\hat{B}_{iii}^{Igg}(\ell_1, \ell_2, \ell_3) = \frac{B_{iii}^{(2)}|_S(\ell_1, \ell_2, \ell_3) - Q_3(\ell_1, \ell_2, \ell_3) B_{iii}^{(2)}(\ell_1, \ell_2, \ell_3)}{1 - Q_3(\ell_1, \ell_2, \ell_3)}. \quad (30)$$

As expected, when $Q_3 = 0$ this gives $\hat{B}_{iii}^{Igg} = B_{iii}^{(2)}|_S$ as for a spectroscopic galaxy sample with no photo-z error. However, Q_3 must not approach unity, where \hat{B}_{iii}^{Igg} is singular. For the LSST-like survey described in Sec. 2.1, we calculate Q_3 for various redshift bins following the procedure described in Sec. 3.3. This result is given in Fig. 2 for equilateral triangles, where

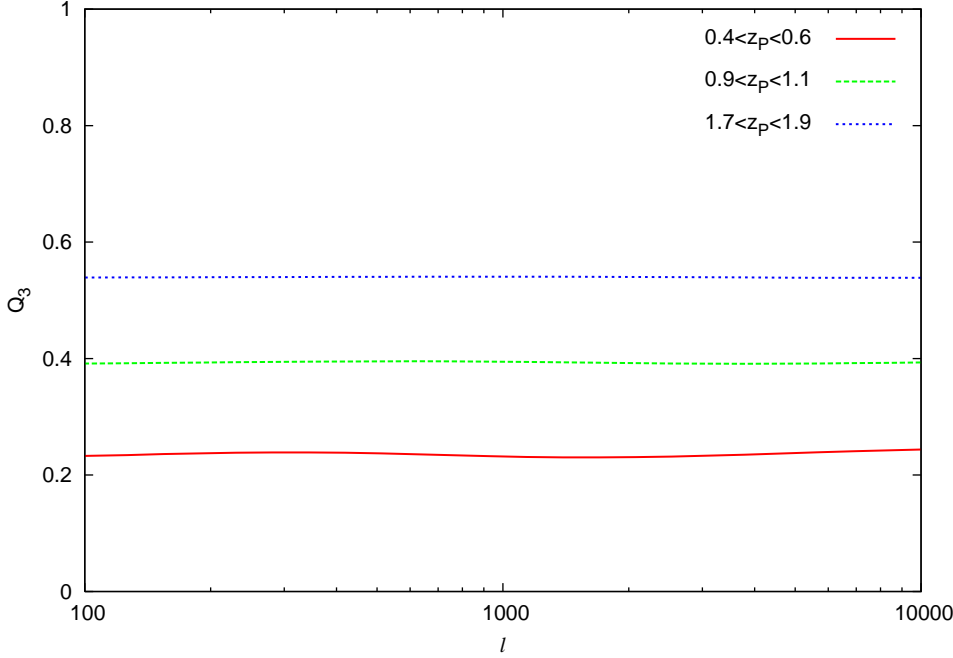


Figure 2. The behavior of $Q_3(\ell_1, \ell_2, \ell_3) \equiv B_{iii}^{Ggg}|_S(\ell_1, \ell_2, \ell_3)/B_{iii}^{Ggg}(\ell_1, \ell_2, \ell_3)$ for equilateral triangles ($\ell = \ell_1 = \ell_2 = \ell_3$) over three redshift bins spanning the survey range. Similar to the 2-point case, the suppression is dependent on the redshift bin chosen, increasing with redshift due to increased photo-z error at higher redshift, but is largely scale independent due to being the ratio of two bispectra. For this reason there is also little dependence on triangle shape. Generally, $Q \approx 0.4$, and the significant deviation from unity ensures that the estimator \hat{B}_{iii}^{Igg} is valid for lensing surveys of interest.

we find $Q_3 \approx 0.4$ and in general that Q_3 should deviate significantly from unity. The estimator \hat{B}_{iii}^{Igg} is thus expected to be applicable in any typical lensing survey.

3.3 Evaluating $Q_3(\ell_1, \ell_2, \ell_3)$

In order to evaluate the ratio Q_3 in Eq. 28, we will begin from the real space angular correlation function $w^{Ggg'}(\theta_1, \theta_2, \theta_3; z_G^P, z_g^P, z_{g'}^P)$ between shear at photo-z z_G^P and galaxy density at photo-z z_g^P and $z_{g'}^P$. The average correlation over the distribution of galaxies in the i -th redshift bin is

$$\begin{aligned}
 w_{iii}^{Ggg'}(\theta_1, \theta_2, \theta_3) &= \int_i dz_G^P \int_i dz_g^P \int_i dz_{g'}^P w^{Ggg'}(\theta_1, \theta_2, \theta_3; z_G^P, z_g^P, z_{g'}^P) n_i^P(z_G^P) n_i^P(z_g^P) n_i^P(z_{g'}^P) \\
 &= \int_i dz_G^P \int_i dz_g^P \int_i dz_{g'}^P \int_0^\infty dz_G \int_0^\infty dz_g \int_0^\infty dz_{g'} w^{Ggg'}(\theta_1, \theta_2, \theta_3; z_G, z_g, z_{g'}) \\
 &\quad \times p(z_G|z_G^P) p(z_g|z_g^P) p(z_{g'}|z_{g'}^P) n_i^P(z_G^P) n_i^P(z_g^P) n_i^P(z_{g'}^P),
 \end{aligned} \tag{31}$$

where we have used the shorthand $\int_i = \int_{z_i - \Delta z_i/2}^{z_i + \Delta z_i/2}$ to represent integration over the i -th redshift bin. In terms of the ensemble average $\langle \dots \rangle$, which is in practice an average over θ' , the angular real space correlation function is

$$w^{Ggg'}(\theta_1, \theta_2, \theta_3; z_G, z_g, z_{g'}) = \int_0^\infty dz_L \langle \delta_m(\theta'; z_G) \delta_g(\theta' + \theta_2; z_g) \delta_g(\theta' + \theta_3; z_{g'}) \rangle W_L(z_L, z_G) \delta^D(\theta_1 + \theta_2 + \theta_3), \tag{32}$$

where $\delta^D(\theta_1 + \theta_2 + \theta_3)$ ensures that the three vectors form a triangle. We can now write Eq. 31 as

$$\begin{aligned}
 w_{iii}^{Ggg'}(\theta_1, \theta_2, \theta_3) &= \int_i dz_G^P \int_i dz_g^P \int_i dz_{g'}^P \int_0^\infty dz_G \int_0^\infty dz_g \int_0^\infty dz_{g'} \int_0^\infty dz_L \langle \delta_m(\theta'; z_G) \delta_g(\theta' + \theta_2; z_g) \delta_g(\theta' + \theta_3; z_{g'}) \rangle \\
 &\quad \times \delta^D(\theta_1 + \theta_2 + \theta_3) W_L(z_L, z_G) p(z_G|z_G^P) p(z_g|z_g^P) p(z_{g'}|z_{g'}^P) n_i^P(z_G^P) n_i^P(z_g^P) n_i^P(z_{g'}^P) \\
 &= \int_0^\infty dz_L \int_0^\infty dz_g \int_0^\infty dz_{g'} \langle \delta_m(\theta'; z_G) \delta_g(\theta' + \theta_2; z_g) \delta_g(\theta' + \theta_3; z_{g'}) \rangle \delta^D(\theta_1 + \theta_2 + \theta_3) \\
 &\quad \times W_i(z_L) n_i(z_g) n_i(z_{g'}).
 \end{aligned} \tag{33}$$

The second correlation function needed is identical to Eq. 33, but takes the average over all triplets such that $z_G^P < z_g^P, z_{g'}^P$,

$$w_{iii}^{Ggg'}|_S(\theta_1, \theta_2, \theta_3) = \int_0^\infty dz_L \int_0^\infty dz_g \int_0^\infty dz_{g'} \langle \delta_m(\theta'; z_G) \delta_g(\theta' + \theta_2; z_g) \delta_g(\theta' + \theta_3; z_{g'}) \rangle \delta^D(\theta_1 + \theta_2 + \theta_3) \\ \times W_i(z_L) n_i(z_g) n_i(z_{g'}) \eta(z_L, z_g, z_{g'}). \quad (34)$$

We have used here

$$\eta(z_L, z_g, z_{g'}) = \frac{3 \int_i dz_G^P \int_i dz_g^P \int_i dz_{g'}^P \int_0^\infty dz_G W_L(z_L, z_G) p(z_G|z_G^P) p(z_g|z_g^P) p(z_{g'}|z_{g'}^P) n_i^P(z_G^P) n_i^P(z_g^P) n_i^P(z_{g'}^P) S(z_G^P, z_g^P, z_{g'}^P)}{\int_i dz_G^P \int_i dz_g^P \int_i dz_{g'}^P \int_0^\infty dz_G W_L(z_L, z_G) p(z_G|z_G^P) p(z_g|z_g^P) p(z_{g'}|z_{g'}^P) n_i^P(z_G^P) n_i^P(z_g^P) n_i^P(z_{g'}^P)}, \quad (35)$$

where $S(z_G^P, z_g^P, z_{g'}^P) = 1$ if $z_G^P < z_g^P, z_{g'}^P$ and is zero otherwise. Since $S(z_G^P, z_g^P, z_{g'}^P)$ allows only 1/3 of the integral to survive, $\eta(z_L, z_g, z_{g'})$ is normalised by a factor 3 in order to remove the suppression due to the selection function and measure only that due to the lensing geometry. This is demonstrated by the relation

$$\frac{\int_i dz_G^P \int_i dz_g^P \int_i dz_{g'}^P \int_0^\infty dz_G p(Z_G|z_G^P) p(Z_g|z_g^P) p(Z_{g'}|z_{g'}^P) n_i^P(z_G^P) n_i^P(z_g^P) n_i^P(z_{g'}^P) S(z_G^P, z_g^P, z_{g'}^P)}{\int_i dz_G^P \int_i dz_g^P \int_i dz_{g'}^P \int_0^\infty dz_G p(Z_G|z_G^P) p(Z_g|z_g^P) p(Z_{g'}|z_{g'}^P) n_i^P(z_G^P) n_i^P(z_g^P) n_i^P(z_{g'}^P)} = \frac{1}{3}. \quad (36)$$

We now take the Fourier transform of Eqs. 33 & 34 to find the bispectra B_{iii}^{Ggg} and $B_{iii}^{Ggg}|_S$, respectively. Again following the Limber approximation, with dominant correlation at $z_L = z_g = z_{g'}$, we have

$$B_{iii}^{Ggg}(\ell_1, \ell_2, \ell_3) = \int_0^\infty B^{Ggg}(k_1, k_2, k_3; \chi) \frac{W_i(\chi) f_i^2(\chi)}{\chi^4} d\chi \quad (37)$$

and

$$B_{iii}^{Ggg}|_S(\ell_1, \ell_2, \ell_3) = \int_0^\infty B^{Ggg}(k_1, k_2, k_3; \chi) \frac{W_i(\chi) f_i^2(\chi)}{\chi^4(z)} \eta(\chi, \chi(z_g) = \chi, \chi(z_{g'}) = \chi) d\chi. \quad (38)$$

The ratio Q_3 is now expressed directly through Eqs. 37 & 38. We can approximate $Q_3 \approx \bar{\eta}_i$, where $\bar{\eta}_i$ is the mean value of η across the i -th redshift bin, since the integrals differ only by a factor η . η has the same dependence as Q_3 on the relative contribution to the Ggg correlation from triplets with $z_G^P < z_g^P, z_{g'}^P$ compared to triplets with other relative orientations. In the limit where photo-z error dominates, $\sigma_P \gg \Delta z$, and there is no suppression of the contribution to the Ggg correlation by the selection function, so $\eta, Q_3 \rightarrow 1$. In this limit, the estimator \hat{B}_{iii}^{Igg} becomes singular and B_{iii}^{Igg} can no longer be differentiated from B_{iii}^{Ggg} . In the opposite limit, where $\sigma_P \ll \Delta z$, the selection function suppresses all contribution to the Ggg correlation and $\eta, Q_3 \rightarrow 0$, where our estimator mirrors the extraction method for B_{iii}^{Igg} in spectroscopic galaxy samples.

4 PERFORMANCE OF THE GGI SELF-CALIBRATION

In order to evaluate the statistical and systematic errors in the GGI self-calibration, we calculate directly the power spectra and bispectra through the Limber approximation according to the anticipated survey parameters discussed in Sec. 2.1. For the bispectra, we employ the fitting formula of Scoccimarro & Couchman (2001) for the 3D matter density bispectrum due to non-linear clustering. We modify this as described in Sec. 3.1 for the 3D galaxy bispectrum, using values for the galaxy bias of $b_1^i = 1.0$ and $b_2^i = -0.1$ (Simpson et al. 2011). We include the intrinsic alignment correlations of B^{IGG} and B^{Igg} in a straightforward manner following the linear alignment model of Hirata & Seljak (2004), where $P_{\delta, \gamma I} = -\frac{C_1 \bar{p}}{D(z)(1+z)} P_\delta$. Like Bridle & King (2007), we extend this to the non-linear matter power spectrum for use in the fitting formula, where C_1 is estimated by comparison to Fig. 2 of Hirata & Seljak (2004).

4.1 The estimation of B_{iii}^{Igg}

In order to quantify the accuracy of the estimator $\hat{B}_{iii}^{Igg}(\ell_1, \ell_2, \ell_3)$, we consider the contribution of measurement errors such as shot and shape noise in $\hat{B}_{iii}^{(2)}(\ell_1, \ell_2, \ell_3)$ which propagate into our measurement of $B_{iii}^{Igg}(\ell_1, \ell_2, \ell_3)$ through the estimator. We calculate the rms error for a given redshift bin, working in a pixel space with N_P sufficiently fine and uniform pixels of photo-z with bin width Δz and angular position with bin width $\Delta \ell$. Each pixel is associated with a photo-z z_α^P , angular position θ_α , measured overdensity $\delta_\alpha + \delta_\alpha^N$ and measured ‘shear’ $\kappa_\alpha + \kappa_\alpha^I + \kappa_\alpha^N$, where ‘N’ represents the measurement noise. From Eq. 29, we construct the pixel space angular bispectra

$$\begin{aligned}
B^{(2)}(\ell_1, \ell_2, \ell_3) &= N_P^{-3} \sum_{\alpha\beta\gamma} [\delta_\alpha + \delta_\alpha^N][\delta_\beta + \delta_\beta^N][\kappa_\gamma + \kappa_\gamma^I + \kappa_\gamma^N] \exp[i(\ell_1 \cdot \boldsymbol{\theta}_\alpha + \ell_2 \cdot \boldsymbol{\theta}_\beta + \ell_3 \cdot \boldsymbol{\theta}_\gamma)], \\
B^{(2)}|_S(\ell_1, \ell_2, \ell_3) &= N_P^{-3} \sum_{\alpha\beta\gamma} [\delta_\alpha + \delta_\alpha^N][\delta_\beta + \delta_\beta^N][\kappa_\gamma + \kappa_\gamma^I + \kappa_\gamma^N] \exp[i(\ell_1 \cdot \boldsymbol{\theta}_\alpha + \ell_2 \cdot \boldsymbol{\theta}_\beta + \ell_3 \cdot \boldsymbol{\theta}_\gamma)] S_{\alpha\beta\gamma}.
\end{aligned} \tag{39}$$

$S_{\alpha\beta\gamma} = 1$ when $z_\alpha^P, z_\beta^P > z_\gamma^P$ and is zero otherwise. Thus in the limit $N_P \gg 1$, $\sum_{\alpha\beta\gamma} S_{\alpha\beta\gamma} = N_P^3/3$ and the average $\bar{S}_{\alpha\beta\gamma} = 1/3$. From our definition of the estimator in Eq. 30, we can construct the difference

$$\begin{aligned}
\hat{B}_{iii}^{Igg} - B_{iii}^{Igg} &= \frac{1}{(1-Q_3)} N_P^{-3} \sum_{\alpha\beta\gamma} \exp[i(\ell_1 \cdot \boldsymbol{\theta}_\alpha + \ell_2 \cdot \boldsymbol{\theta}_\beta + \ell_3 \cdot \boldsymbol{\theta}_\gamma)] [(\delta_\alpha + \delta_\alpha^N)(\delta_\beta + \delta_\beta^N)(\kappa_\gamma + \kappa_\gamma^I + \kappa_\gamma^N)(3S_{\alpha\beta\gamma} - Q_3) \\
&\quad - (1-Q_3)\delta_\alpha\delta_\beta\kappa_\gamma^I] \\
&= \frac{1}{(1-Q_3)} N_P^{-3} \sum_{\alpha\beta\gamma} \exp[i(\ell_1 \cdot \boldsymbol{\theta}_\alpha + \ell_2 \cdot \boldsymbol{\theta}_\beta + \ell_3 \cdot \boldsymbol{\theta}_\gamma)] [(\delta_\alpha\delta_\beta^N + \delta_\alpha^N\delta_\beta + \delta_\alpha^N\delta_\beta^N)(\kappa_\gamma + \kappa_\gamma^I + \kappa_\gamma^N) + \delta_\alpha\delta_\beta(\kappa_\gamma + \kappa_\gamma^N)] \\
&\quad \times (3S_{\alpha\beta\gamma} - Q_3).
\end{aligned} \tag{40}$$

Here we have used $\bar{S}_{\alpha\beta\gamma} = 1/3$ and that the ggl correlation doesn't depend on the relative position of the galaxy triplets. The rms error is

$$\begin{aligned}
(\Delta B_{iii}^{Igg})^2 &= \frac{1}{(1-Q_3)^2} N_P^{-6} \sum_{\alpha\beta\gamma} \sum_{\lambda\mu\nu} \exp[i(\ell_1 \cdot \boldsymbol{\theta}_\alpha + \ell_2 \cdot \boldsymbol{\theta}_\beta + \ell_3 \cdot \boldsymbol{\theta}_\gamma)] \exp[i(\ell_1 \cdot \boldsymbol{\theta}_\lambda + \ell_2 \cdot \boldsymbol{\theta}_\mu + \ell_3 \cdot \boldsymbol{\theta}_\nu)] (3S_{\alpha\beta\gamma} - Q_3) \\
&\quad \times (3S_{\lambda\mu\nu} - Q_3) [(\delta_\alpha\delta_\beta^N + \delta_\alpha^N\delta_\beta + \delta_\alpha^N\delta_\beta^N)(\kappa_\gamma + \kappa_\gamma^I + \kappa_\gamma^N) + \delta_\alpha\delta_\beta(\kappa_\gamma + \kappa_\gamma^N)] \\
&\quad \times [(\delta_\lambda\delta_\mu^N + \delta_\lambda^N\delta_\mu + \delta_\lambda^N\delta_\mu^N)(\kappa_\nu + \kappa_\nu^I + \kappa_\nu^N) + \delta_\lambda\delta_\mu(\kappa_\nu + \kappa_\nu^N)],
\end{aligned} \tag{41}$$

where $\langle \dots \rangle$ is the ensemble average. The ensemble average is over 121 terms of the form $\langle ABCDEF \rangle$, $A, B, C, D, E, F \in \delta, \delta^N, \kappa, \kappa^I, \kappa^N$. To simplify this we apply Wick's theorem for the 6-point correlation,

$$\langle ABCDEF \rangle = \langle AB \rangle \langle CD \rangle \langle EF \rangle + \langle AB \rangle \langle CE \rangle \langle DF \rangle + (14 \text{ perm.}). \tag{42}$$

This results in 1815 products of three 2-point correlations, most of which are zero. Any correlation between signal and noise or dissimilar noise terms vanish. Due to the angular dependence of the correlations ($\langle A_a B_b \rangle = w_{AB}(\theta_a - \theta_b)$), only those correlations with $\langle A_a B_b \rangle$ where $a \in \alpha, \beta, \gamma$ and $b \in \lambda, \mu, \nu$ are non-vanishing. This leaves 42 surviving products:

$$\begin{aligned}
(\Delta B_{iii}^{Igg})^2 &= \frac{1}{(1-Q_3)^2} N_P^{-6} \sum_{\alpha\beta\gamma} \sum_{\lambda\mu\nu} \exp[i(\ell_1 \cdot \boldsymbol{\theta}_\alpha + \ell_2 \cdot \boldsymbol{\theta}_\beta + \ell_3 \cdot \boldsymbol{\theta}_\gamma)] \exp[i(\ell_1 \cdot \boldsymbol{\theta}_\lambda + \ell_2 \cdot \boldsymbol{\theta}_\mu + \ell_3 \cdot \boldsymbol{\theta}_\nu)] (3S_{\alpha\beta\gamma} - Q_3) \\
&\quad \times (3S_{\lambda\mu\nu} - Q_3) [(\delta_\alpha\delta_\lambda) [(\delta_\beta\delta_\mu) + \langle \delta_\beta^N \delta_\mu^N \rangle] (\langle \kappa_\gamma \kappa_\nu \rangle + \langle \kappa_\gamma^N \kappa_\nu^N \rangle) + \langle \delta_\beta^N \delta_\mu^N \rangle \langle \kappa_\gamma^I \kappa_\nu^I \rangle + \langle \kappa_\gamma \delta_\mu \rangle \langle \delta_\beta \kappa_\nu \rangle] \\
&\quad + \langle \delta_\alpha \delta_\mu \rangle [(\delta_\beta\delta_\lambda) + \langle \delta_\beta^N \delta_\lambda^N \rangle] (\langle \kappa_\gamma \kappa_\nu \rangle + \langle \kappa_\gamma^N \kappa_\nu^N \rangle) + \langle \delta_\beta^N \delta_\lambda^N \rangle \langle \kappa_\gamma^I \kappa_\nu^I \rangle + \langle \kappa_\gamma \delta_\lambda \rangle \langle \delta_\beta \kappa_\nu \rangle] \\
&\quad + \langle \delta_\alpha^N \delta_\lambda^N \rangle [(\delta_\beta\delta_\mu) + \langle \delta_\beta^N \delta_\mu^N \rangle] (\langle \kappa_\gamma \kappa_\nu \rangle + \langle \kappa_\gamma^N \kappa_\nu^N \rangle + \langle \kappa_\gamma^I \kappa_\nu^I \rangle) + \langle (\kappa_\gamma + I_\gamma) \delta_\mu \rangle \langle \delta_\beta (\kappa_\nu + \kappa_\nu^I) \rangle] \\
&\quad + \langle \delta_\alpha^N \delta_\mu^N \rangle [(\delta_\beta\delta_\lambda) + \langle \delta_\beta^N \delta_\lambda^N \rangle] (\langle \kappa_\gamma \kappa_\nu \rangle + \langle \kappa_\gamma^N \kappa_\nu^N \rangle + \langle \kappa_\gamma^I \kappa_\nu^I \rangle) + \langle (\kappa_\gamma + \kappa_\gamma^I) \delta_\lambda \rangle \langle \delta_\beta (\kappa_\nu + I_\nu) \rangle] \\
&\quad + \langle \delta_\alpha \kappa_\nu \rangle [\langle \delta_\beta \delta_\mu \rangle \langle \kappa_\gamma \delta_\lambda \rangle + \langle \delta_\beta \delta_\lambda \rangle \langle \kappa_\gamma \delta_\mu \rangle] + \langle \delta_\alpha (\kappa_\nu + \kappa_\nu^I) \rangle [\langle \delta_\beta^N \delta_\mu^N \rangle \langle (\kappa_\gamma + \kappa_\gamma^I) \delta_\lambda \rangle + \langle \delta_\beta^N \delta_\lambda^N \rangle \langle (\kappa_\gamma + \kappa_\gamma^I) \delta_\mu \rangle].
\end{aligned}$$

Noises only correlate at zero lag ($\langle \delta_\alpha^N \delta_\lambda^N \rangle \propto \delta_{\alpha\lambda}$, $\langle \kappa_\gamma^N \kappa_\nu^N \rangle \propto \delta_{\gamma\nu}$), and the correlations $\langle \delta\delta \rangle$, $\langle \delta\kappa^I \rangle$, $\langle \kappa\kappa \rangle$ and $\langle \kappa^I \kappa^I \rangle$ depend only on separation, not on relative orientation of the galaxy pairs along the line-of-sight. However, $\langle \kappa\delta \rangle$ is dependent on the relative orientation along the line-of-sight and must be treated with care when evaluating Eq. 43. In order to quantify this orientation dependence, we apply Q_2 such that

$$\langle \delta_\alpha \kappa_\nu \rangle \rightarrow \frac{1}{2} \left(\frac{S_{\alpha\nu}}{(1-Q_2)} + \frac{S_{\nu\alpha}}{Q_2} \right) \langle \delta_\alpha \kappa_\nu \rangle. \tag{44}$$

We can now evaluate Eq. 43 analytically, taking the Fourier transform to find

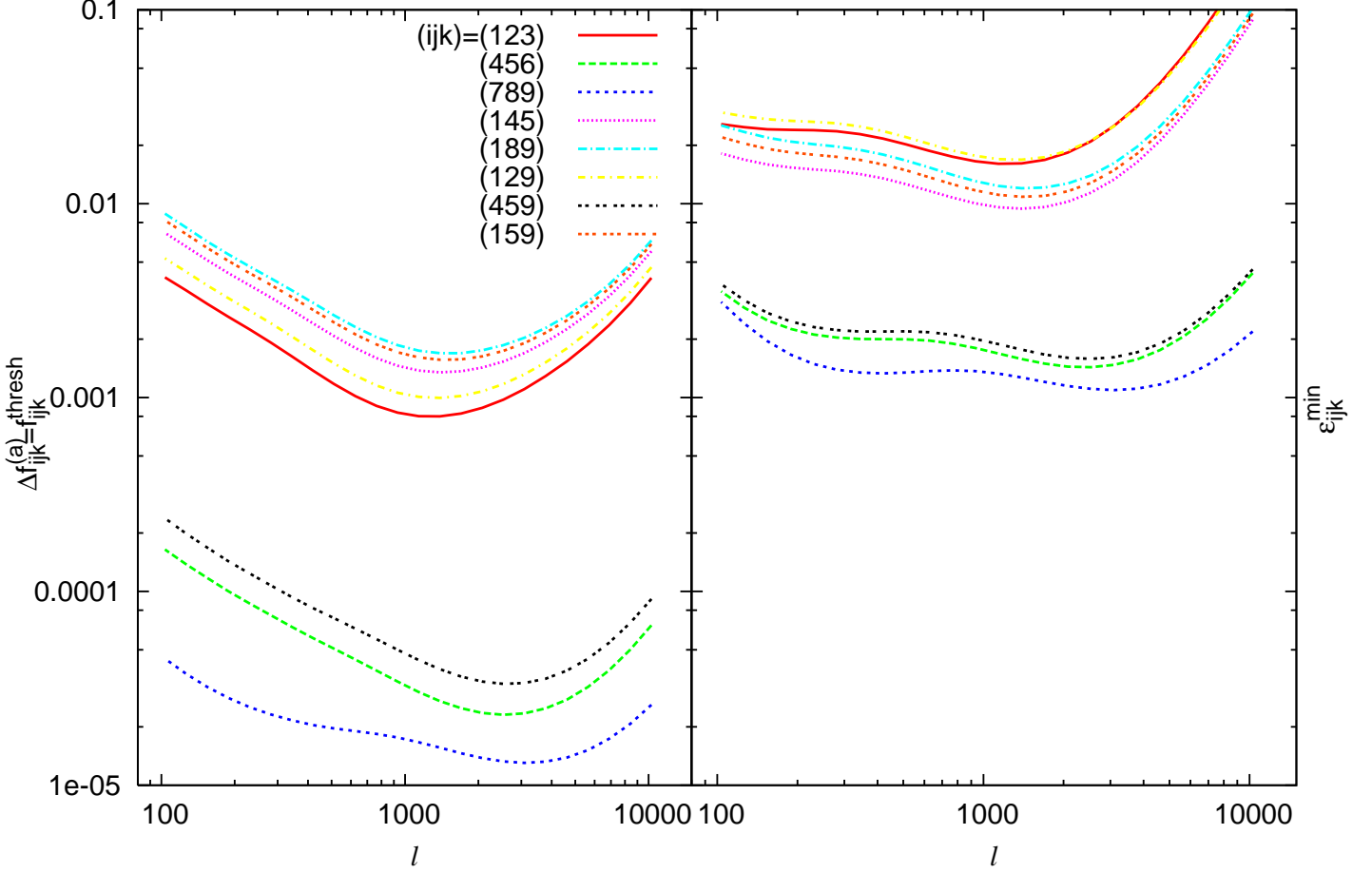


Figure 3. Left: The residual statistical uncertainty $\Delta f_{ijk}^{(a)}$ in the B_{ijk}^{IGG} measurement and threshold of intrinsic alignment contamination f_{ijk}^{thresh} at which the GGI self-calibration technique can calculate and remove the intrinsic alignment contamination at $S/N=1$ are plotted for a variety of redshift bin combinations. Right: The minimum measurement error ϵ_{ijk}^{min} for B_{ijk}^{GGG} is plotted for comparison. Both errors are plotted for equilateral triangles ($\ell = \ell_1 = \ell_2 = \ell_3$) and have a similar ℓ dependence, with the effects of shot noise taking over at large ℓ . Generally, $\Delta f_{ijk}^{(a)} < \epsilon_{ijk}^{min}$, and is thus negligible. We expect this result to hold for non-equilateral triangles as well, but the use of the GGI self-calibration is limited by our understanding of non-Gaussian effects for very elongated triangle shapes, as discussed in Sec. 4.4, and we leave discussion of its applicability for these very elongated triangle shapes to a future work.

$$\begin{aligned}
 (\Delta B_{iii}^{Igg})^2 &= 2 \left\{ \left(C_{ii}^{GG} C_{ii}^{gg} + b C_{ii}^{GG,N} C_{ii}^{gg} + 2f C_{ii}^{gG} C_{ii}^{gG} \right) C_{ii}^{gg} \right. \\
 &\quad + 2 \left(a \left[\left(C_{ii}^{GG} + C_{ii}^{II} \right) C_{ii}^{gg} + C_{ii}^{gI} C_{ii}^{gI} \right] + d C_{ii}^{GG,N} C_{ii}^{gg} + g C_{ii}^{gG} C_{ii}^{gG} + 2h C_{ii}^{gG} C_{ii}^{gI} \right. \\
 &\quad \left. \left. + \left[c \left(C_{ii}^{GG} + C_{ii}^{II} \right) + e C_{ii}^{GG,N} \right] C_{ii}^{gg,N} \right) C_{ii}^{gg,N} \right\}. \tag{45}
 \end{aligned}$$

The details of this calculation and the coefficients $a - h$ are found in the Appendix.

The final rms error ΔB_{iii}^{Igg} evaluated for a given triangle with bin width $\Delta\ell$ is then given by

$$\begin{aligned}
 (\Delta B_{iii}^{Igg})^2 &= \frac{4\pi^2}{\ell_1 \ell_2 \ell_3 \Delta\ell_1 \Delta\ell_2 \Delta\ell_3 f_{sky}} \left\{ \left(C_{ii}^{GG} C_{ii}^{gg} + b C_{ii}^{GG,N} C_{ii}^{gg} + 2f C_{ii}^{gG} C_{ii}^{gG} \right) C_{ii}^{gg} \right. \\
 &\quad + 2 \left(a \left[\left(C_{ii}^{GG} + C_{ii}^{II} \right) C_{ii}^{gg} + C_{ii}^{gI} C_{ii}^{gI} \right] + d C_{ii}^{GG,N} C_{ii}^{gg} + g C_{ii}^{gG} C_{ii}^{gG} + 2h C_{ii}^{gG} C_{ii}^{gI} \right. \\
 &\quad \left. \left. + \left[c \left(C_{ii}^{GG} + C_{ii}^{II} \right) + e C_{ii}^{GG,N} \right] C_{ii}^{gg,N} \right) C_{ii}^{gg,N} \right\}. \tag{46}
 \end{aligned}$$

$C_{ii}^{gg,N} = 1/\bar{n}_i$ and $C_{ii}^{GG,N} = \gamma_{rms}^2/\bar{n}_i$, where \bar{n}_i is the average number density of galaxies in the i -th redshift bin. Unlike the GI self-calibration, ΔB_{iii}^{Igg} is dependent on the intrinsic alignment contamination through C_{ii}^{gI} . However, it is still insensitive to the intrinsic alignment contamination in the limit where C_{ii}^{GG} is dominant.

The errors ΔB_{iii}^{Igg} and ΔC_{ii}^{Ig} propagate into the measurement of B_{ijk}^{IGG} through Eq. 27. Performing a standard error propagation gives a residual statistical error ΔB_{ijk}^{IGG} . For the equilateral case, this simplifies to

$$\begin{aligned} \left(\Delta B_{ijk}^{IGG}(\ell)\right)^2 &= \left(\frac{W_{ijk}}{(b_1^i)^2 \Pi_{iii}}\right)^2 \left(\Delta B_{iii}^{Igg}(\ell)\right)^2 + \left(\frac{b_2^i W_{ijk}}{(b_1^i)^3 \Pi_{ii} \omega_{ii}}\right)^2 \\ &\times \left[\left(2C_{ii}^{GG}(\ell) \Delta C_{ii}^{Ig}(\ell)\right)^2 + \left(2C_{ii}^{Ig}(\ell) C_{ii}^{GG,N}(\ell)\right)^2 + \left(\frac{\omega_{ii}}{b_1^i \Pi_{ii}}\right)^2 \left(2C_{ii}^{Ig}(\ell) \Delta C_{ii}^{Ig}(\ell)\right)^2 \right], \end{aligned} \quad (47)$$

where we have neglected terms of order Δ^2 . To find the fractional error $\Delta f_{ijk}^{(a)}$ this induces in the lensing bispectrum, we simply scale ΔB_{ijk}^{IGG} by the factor f_{ijk}^I such that $\Delta f_{ijk}^{(a)} = f_{ijk}^I \Delta B_{ijk}^{IGG}$. Like the 2-point case, this error is equal to f_{ijk}^{thresh} , the minimum intrinsic alignment f_{ijk}^I which can be detected through the self-calibration with $S/N=1$ or $\Delta B_{iii}^{Igg} = B_{iii}^{Igg}$. Thus $f_{ijk}^{thresh} = \Delta f_{ijk}^{(a)}$ represents for the self-calibration both the residual statistical error in the measurement of C_{ijk}^{GGG} and the lower limit at which the intrinsic alignment can be calculated and removed. The GGI self-calibration technique can then turn a systematic contamination f_{ijk}^I of the lensing signal into a statistical error $\Delta f_{ijk}^{(a)} < f_{ijk}^I$ which is insensitive to the original intrinsic alignment contamination.

We compare the error $\Delta f_{ijk}^{(a)}$ to the minimum rms error due to cosmic variance and shot noise in the B_{ijk}^{GGG} measurement, which ignores other sources of error like the intrinsic alignment. The rms error of B_{ijk}^{GGG} ($i \neq j \neq k$) is

$$\begin{aligned} \left(\Delta B_{ijk}^{GGG}\right)^2 &= \left(C_{ii}^{GG} + C_{ii}^{GG,N}\right) \left(C_{jj}^{GG} + C_{jj}^{GG,N}\right) \left(C_{kk}^{GG} + C_{kk}^{GG,N}\right) + \left(C_{ii}^{GG} + C_{ii}^{GG,N}\right) C_{jk}^{GG} C_{jk}^{GG} \\ &+ \left(C_{jj}^{GG} + C_{jj}^{GG,N}\right) C_{ik}^{GG} C_{ik}^{GG} + \left(C_{kk}^{GG} + C_{kk}^{GG,N}\right) C_{ij}^{GG} C_{ij}^{GG} + 2C_{ij}^{GG} C_{jk}^{GG} C_{ik}^{GG}. \end{aligned} \quad (48)$$

This gives an absolute lower limit on the fractional measurement error of

$$\left(\epsilon_{ijk}^{min}\right)^2 = \frac{2\pi^2}{\ell_1 \ell_2 \ell_3 \Delta \ell_1 \Delta \ell_2 \Delta \ell_3 f_{sky}} \left(\frac{\Delta B_{ijk}^{GGG}}{B_{ijk}^{GGG}}\right)^2. \quad (49)$$

Where $\Delta f_{ijk}^{(a)} < \epsilon_{ijk}$, the residual measurement error introduced after the GGI self-calibration is negligible, with very little loss of cosmological information. We find this to be true for an LSST-like survey, as shown in Fig. 3. More generally, since $\Delta f_{ijk}^{(a)}$ and ϵ_{ijk} scale similarly with respect to survey parameters, this should hold for other lensing surveys as well.

4.2 The accuracy of the B_{ijk}^{IGG} - B_{iii}^{Igg} relation

In addition to the measurement error introduced through the estimator \hat{B}_{iii}^{Igg} , there is a systematic error which is introduced by Eq. 27, which relates the intrinsic alignment contamination B_{ijk}^{IGG} in the lensing bispectrum to other survey observables. The accuracy of Eq. 27 is quantified by

$$\begin{aligned} \epsilon_{ijk}^{sys} &\equiv \left(\frac{W_{ijk}}{(b_1^i)^2 \Pi_{iii}} \frac{B_{iii}^{Igg}(\ell_1, \ell_2, \ell_3)}{B_{ijk}^{IGG}(\ell_1, \ell_2, \ell_3)} - \frac{b_2^i}{(b_1^i)^2} \frac{W_{ijk}}{\omega_{ii} \Pi_{ii}} \frac{1}{B_{ijk}^{IGG}(\ell_1, \ell_2, \ell_3)} \right. \\ &\times \left. \left[C_{ii}^{Ig}(\ell_1) C_{ii}^{GG}(\ell_2) + C_{ii}^{GG}(\ell_2) C_{ii}^{Ig}(\ell_3) + \frac{\omega_{ii}}{b_1^i \Pi_{ii}} C_{ii}^{Ig}(\ell_1) C_{ii}^{Ig}(\ell_3) \right] \right)^{-1} - 1. \end{aligned} \quad (50)$$

This induces a residual systematic error in the lensing measurement of

$$\delta f_{ijk} = \epsilon_{ijk}^{sys} f_{ijk}^I. \quad (51)$$

ϵ_{ijk}^{sys} is evaluated numerically and shown in Fig. 4 for equilateral triangles. As in the 2-point case, Eq. 27 is most accurate for those galaxy triplets which do not share neighbouring redshift bins. In the cases of neighboring bins, the lensing kernel varies more quickly due to the proximity of the galaxies in redshift. This causes Eq. 27 to be less accurate, increasing the systematic error. For galaxy triplets with bins which are not adjacent, $|\epsilon_{ijk}^{sys}| < 0.1$. For these bin choices, the intrinsic alignment contamination can be suppressed by a factor of 10 or greater. In most cases where two or three bins are adjacent, $|\epsilon_{ijk}^{sys}| < 0.2$, which allows for a suppression in the contamination by a factor of 5-10. In only a few of the cases where all three bins are adjacent is $|\epsilon_{ijk}^{sys}| > 0.2$, and even in these cases we expect a suppression in the contamination by a factor of 3 or more. These results are insensitive to the original intrinsic alignment contamination, such that for any $f_{ijk}^{thresh} < f_{ijk}^I < 1$, the GGI self-calibration will reduce the GGI contamination down to survey limits or by a factor of 5-10 or greater, whichever is less, for all but a few redshift bin triplets.

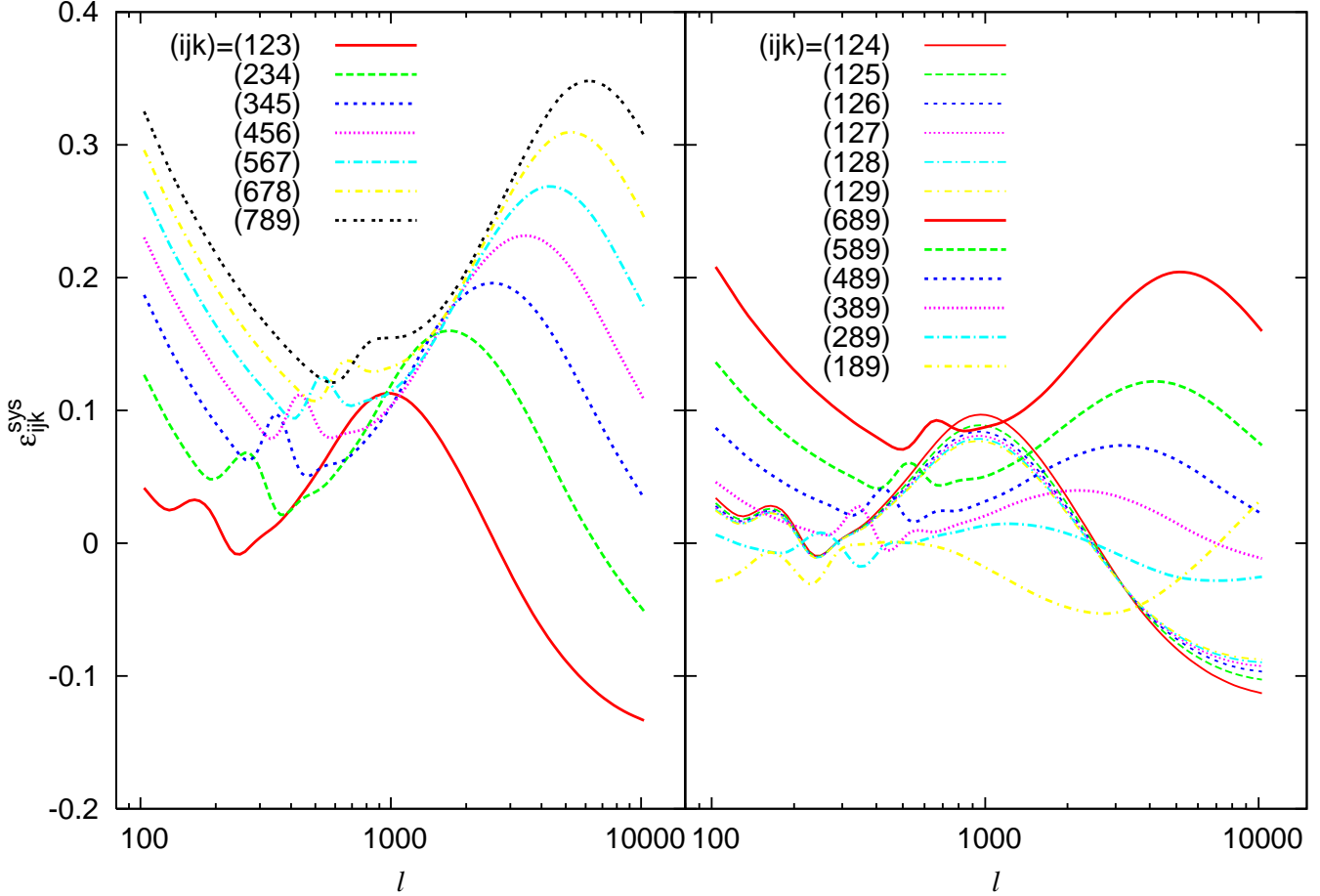


Figure 4. The inaccuracy of the relationship between B_{ijk}^{IGG} and the observable B_{iii}^{Igg} is quantified in Eq. 50 by ϵ_{ijk}^{sys} . This inaccuracy is the source of the dominant systematic error in the measurement of B_{ijk}^{GGG} due to the GGI self-calibration technique. Left: ϵ_{ijk}^{sys} is plotted for three adjacent redshift bins, where the stronger dependence of the lensing kernel on redshift causes a significantly higher inaccuracy. Right: ϵ_{ijk}^{sys} is plotted for redshift bins of varying distance from each other. As expected, the inaccuracy for these bin choices is generally less than for three adjacent bins. ϵ_{ijk}^{sys} is plotted for equilateral triangles ($\ell = \ell_1 = \ell_2 = \ell_3$) in all cases. Equation 27 is usually accurate to within 20%, except for some adjacent bin choices, where it reaches a maximum of approx. 35%. Despite the inaccuracy of Eq. 27 being greater than for Eq. 8 in the GI self-calibration, the GGI self-calibration is still expected to reduce the GGI intrinsic alignment contamination by a factor of 5-10 or more for all but a few adjacent redshift bin triplets. These results are insensitive to the original intrinsic alignment contamination, such that for any $f_{ijk}^{thresh} < f_{ijk}^I < 1$, the GGI self-calibration will reduce the GGI contamination down to survey limits or by a factor of 5-10 or greater, whichever is less, for all but a few adjacent redshift bin triplets.

4.3 The magnification bias

In addition to distorting the shapes of galaxies, gravitational lensing introduces a magnification bias to the observed galaxy overdensity $\delta_g^L = \delta_g + 2(\alpha - 1)\kappa$, where α is determined by the logarithmic slope of the unlensed galaxy luminosity function. The magnification bias affects all three observable bispectra, but we expect the dominant contribution to occur in $B_{iii}^{(2)}$. Including the average magnification bias in the i -th redshift bin, $m_i = \langle 2(\alpha - 1) \rangle$, Eq. 15 is modified to be

$$B_{iii}^{(2)} = B_{iii}^{Ggg} + B_{iii}^{Igg} + 2m_i (B_{iii}^{GGg} + B_{iii}^{IGg}) + m_i^2 (B_{iii}^{GGG} + B_{iii}^{IGG}). \quad (52)$$

We seek to measure B_{iii}^{Igg} for the GGI self-calibration, so we will examine the effect magnification bias has on this measurement. Applying the estimator in Eq. 28, the bispectra B_{iii}^{Igg} and B_{iii}^{GGG} are unaffected, while the others are suppressed by a factor similar to $(1 - Q_3)$. Thus the estimator acts to measure the dominant combination $B_{iii}^{Igg} + m_i^2 B_{iii}^{GGG}$, where $m_i^2 B_{iii}^{GGG}$ contaminates the B_{iii}^{Igg} measurement. Because the GGI self-calibration depends on the results of the 2-point self-calibration, we will also require the contribution $C_{ii}^{Ig} + m_i C_{ii}^{GG}$ from $C_{ii}^{(2)}$ as discussed by Zhang (2010a).

We cannot remove this contamination with any certainty due to measurement errors on m_i , C_{ii}^{GG} and B_{iii}^{GGG} . The direct estimation of the errors involved is lengthy, so we will instead determine the accuracy to which these measurements must

be made in order for the contribution due to magnification bias to be negligible with respect to other errors in the GGI self-calibration.

We will assume m_i has some measurement error Δm_i , B_{iii}^{GGG} a measurement error ΔB_{iii}^{GGG} and C_{ii}^{GG} a measurement error ΔC_{ii}^{GG} . From Eqs. 27 & 8, the induced measurement error in B_{ijk}^{GGG} is

$$\Delta B_{ijk}^{GGG} = \frac{W_{ijk}}{(b_1^i)^2 \Pi_{iii}} \left(2m_i \Delta m_i B_{iii}^{GGG} + m_i^2 B_{iii}^{GGG} \Delta B_{iii}^{GGG} \right) - \frac{b_2^i W_{ijk}}{(b_1^i)^3 \Pi_{ii}^2} \left(2 \frac{W_{ij}}{\omega_{ii}} + 1 \right) \left(\Delta m_i C_{ii}^{GG} + m_i C_{ii}^{GG} \Delta C_{ii}^{GG} \right)^2. \quad (53)$$

Since we are only interested in the upper limit of this effect, we note that $B_{ijk}^{GGG} > B_{iii}^{GGG}$ for $i < j < k$ and use the reduced bispectrum for equilateral triangles $B_{iii}^{GGG} \equiv 3Q_k C_{ii}^{GG} C_{ii}^{GG}$ to write a simplified expression for the induced fractional error in the B_{ijk}^{GGG} measurement as

$$\begin{aligned} \Delta f_{ijk}^M &< \frac{W_{ijk}}{(b_1^i)^2 \Pi_{iii}} \left(2|m_i \Delta m_i| + m_i^2 \left| \frac{\Delta B_{iii}^{GGG}}{B_{iii}^{GGG}} \right| \right) - \frac{b_2^i W_{ijk}}{3Q_k (b_1^i)^3 \Pi_{ii}^2} \left(2 \frac{W_{ij}}{\omega_{ii}} + 1 \right) \left(|\Delta m_i| + \left| m_i \frac{\Delta C_{ii}^{GG}}{C_{ii}^{GG}} \right| \right)^2 \\ &< O(10^{-4}) \left[\left(2 \left| m_i \frac{\Delta m_i}{0.1} \right| + m_i^2 \left| \frac{\Delta B_{iii}^{GGG}/B_{iii}^{GGG}}{10\%} \right| \right) + \left(\left| \frac{\Delta m_i}{0.1} \right| + \left| m_i \frac{\Delta C_{ii}^{GG}/C_{ii}^{GG}}{10\%} \right| \right)^2 \right]. \end{aligned} \quad (54)$$

The above expression is an upper limit on the magnitude of Δf_{ijk}^M given any choice of i, j, k . For a m_i which is large enough to be non-negligible, we need only require an accuracy in its measurement of $\Delta m_i = 0.1$ and a measurement accuracy for B_{iii}^{GGG} and C_{ii}^{GG} of 10% in order to have $f_{ijk}^M < O(10^{-4})$, which is safely negligible by a factor of 10 compared to the minimum measurement error ϵ_{ijk}^{min} of the lensing bispectrum. As discussed by Zhang, this level of accuracy can likely be accomplished by direct measurement of m_i under the approximation $C_{ii}^{(1)} \approx C_{ii}^{GG}$ (see Eq. 7) if the lensing contamination $C_{ii}^{II} < 10\%$. However, if the II contamination is greater than 10% of the lensing signal, more detailed methods must be employed to achieve a great enough accuracy in the m_i measurement for it to be safely negligible, some of which are discussed by Zhang (2010a).

4.4 Non-Gaussianity and galaxy bias

We are only interested in the bispectrum due to the non-linear evolution of gravitational clustering and the associated intrinsic alignment contamination, leaving the accurate estimation of the bispectrum due to primordial non-Gaussianity to other works. Equation 13 should then include a term B_{ijk}^{NG0} which must be separately accounted for. Similarly, the relation between the 3D matter bispectrum and 3D galaxy bispectrum depends on non-Gaussianity beyond the scale dependent correction $b_1(z) \rightarrow b_1(z) + \Delta b(k, z)$ used in relating the 3D matter power spectrum to the 3D galaxy power spectrum (Jeong & Komatsu 2009). Equation 22 must also include the contributions by non-Gaussianity in the term B_{ijk}^{NG0} and from the trispectrum which we have previously neglected.

The full expression including all non-Gaussian contributions is given in Appendix B of Jeong & Komatsu (2009). However, from Figs. 10-14 of Jeong & Komatsu (2009), it is clear that if we avoid very stretched or elongated triangle shapes that are very sensitive to non-Gaussianity, at the scales of interest in a lensing survey ($10^2 < \ell < 10^4$), the total contribution to the relation by non-Gaussianity as a fraction of the non-linear term is less than 10% for $f_{NL} = 40$ and $g_{NL} = 10^4$. If we accept the smaller values of $f_{NL} = 4$ and $g_{NL} = 100$, this fractional contribution is less than 1%. Thus we can safely ignore the contribution of the non-Gaussianity as a source of error to the relation since it is expected to be on the order of the minimum GG measurement error and less than the systematic error discussed in Sec. 4.2. Future work will better constrain and model the effects of non-Gaussianity, thus allowing its effect to be fully accounted for in the GGI self-calibration.

The linear galaxy bias is discussed by Zhang (2010a), and the error induced by the expected uncertainty in its measurement in the GI self-calibration is demonstrated to be negligible compared to other sources of error. The linear and non-linear galaxy bias terms can be measured simultaneously by using the approach of Fry (1994). Using measurements of C^{gg} and B^{ggg} , we extract the bias information from the relationship

$$B_{iii}^{ggg}(\ell_1, \ell_2, \ell_3) \approx (b_1^i)^3 B_{iii}^{mmm} + (b_1^i)^2 b_2^i (C_{ii}^{mm}(\ell_1)C_{ii}^{mm}(\ell_2) + C_{ii}^{mm}(\ell_2)C_{ii}^{mm}(\ell_3) + C_{ii}^{mm}(\ell_1)C_{ii}^{mm}(\ell_3)), \quad (55)$$

where C^{mm} and B^{mmm} are the angular matter power and bispectrum, weighted identically to galaxies. Equation 55 is the analog to Eq. 22, which includes an intrinsic alignment component. The matter power and bispectrum can be tightly constrained by CMB measurements and then evolved, given a cosmology, to low redshift to predict C^{mm} and B^{mmm} .

Both measurement error in B_{iii}^{ggg} and uncertainties in the predictions of C^{mm} and B^{mmm} will affect the measurement of the linear and non-linear galaxy bias parameters. The non-linear galaxy bias is more difficult to constrain precisely than the linear galaxy bias, with typical measured and expected uncertainties in its measurement of up to $\Delta[b_2^i/(b_2^i)^2] \approx 0.5$ at 1σ confidence (LSST Science Collaborations and LSST Project 2009; Simpson et al. 2011). We use the estimate of Zhang

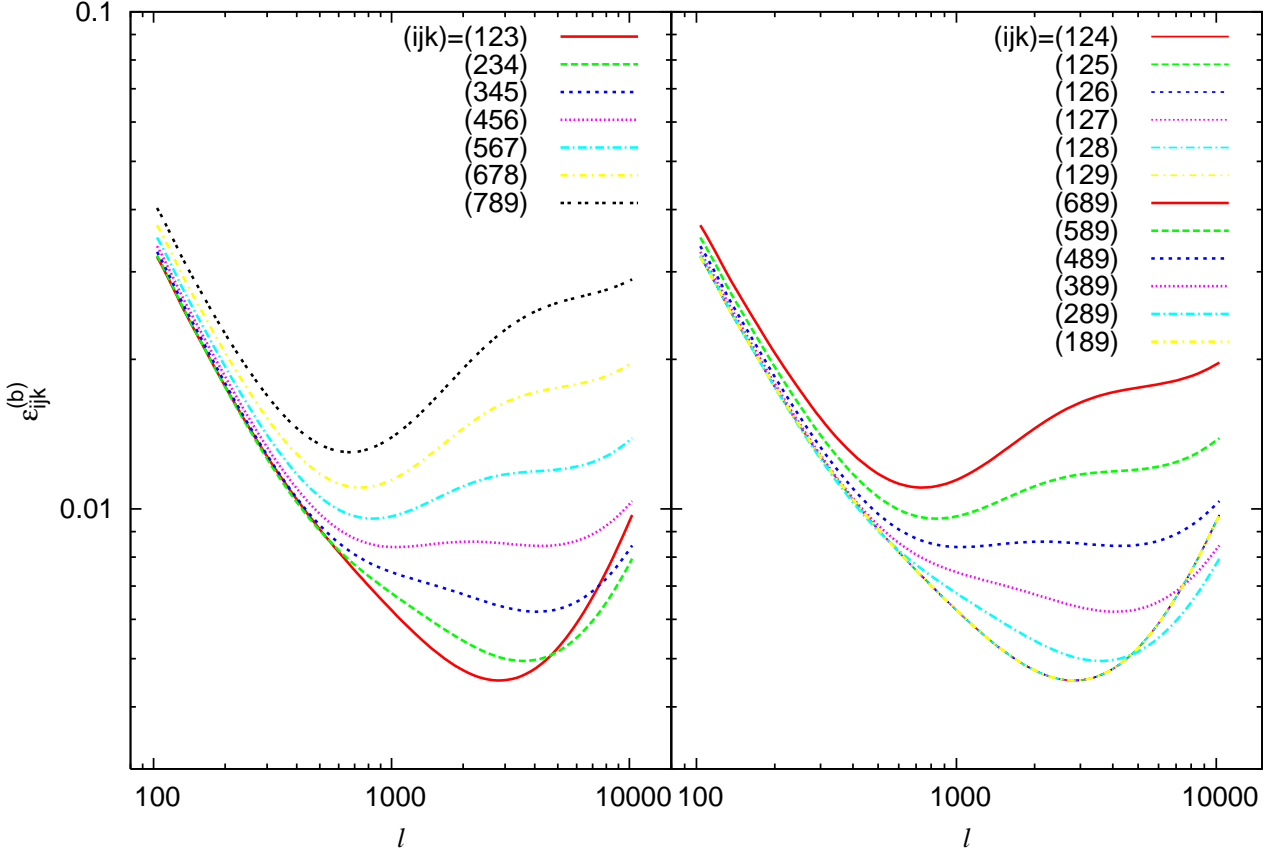


Figure 5. The fractional error $\epsilon_{ijk}^{(b)} = \Delta B^{IGG} / B^{IGG}$ in Eq. 27 is shown for equilateral triangles ($\ell = \ell_1 = \ell_2 = \ell_3$) due to uncertainties in the linear and non-linear galaxy bias. $\epsilon_{ijk}^{(b)}$ is typically less than 2% except for large scales. The measurement error this induces in the final measurement of B^{GGG} , $\Delta f_{ijk}^{(b)} = \epsilon_{ijk}^{(b)} f_{ijk}^I$, is reduced by the factor $f_{ijk}^I \leq 1$. It is thus typically negligible when compared to the minimum measurement error ϵ_{ijk}^{min} in B^{GGG} (Fig. 3).

(2010a) for the measurement error in the linear galaxy bias

$$\frac{\Delta b_1^i}{b_1^i} \approx \frac{1}{2} \sqrt{\frac{1}{\ell \Delta \ell f_{sky}}} \left(1 + \frac{C^{gg,N}}{C^{gg}} \right) \quad (56)$$

to plot in Fig. 5 the fractional error $\epsilon_{ijk}^{(b)} = \Delta B^{IGG} / B^{IGG}$ in Eq. 27 of even a large uncertainty for the non-linear galaxy bias of $\Delta b_2^i \approx 0.5$. We find that $\epsilon_{ijk}^{(b)}$ is generally less than 2% except for large scales. The measurement error this induces in the final measurement of B^{GGG} is then $\Delta f_{ijk}^{(b)} = \epsilon_{ijk}^{(b)} f_{ijk}^I$. Even for very large $f_{ijk}^I = 1$, $\Delta f_{ijk}^{(b)}$ is typically comparable to or less than the minimum measurement error ϵ_{ijk}^{min} in B^{GGG} (Fig. 3). For a typical f_{ijk}^I , we would expect it to be entirely negligible for all bin choices.

The only real limitation which comes from the galaxy bias is then the scale to which it can be applied in the non-linear regime. Recent work (Simpson et al. 2011) has shown that the scale down to which the bias model we have employed is accurate can be extended to $k = 0.5$, which corresponds to $\ell \approx 1000$ at the median redshift of an LSST-like survey. Future work may extend this range further, but for now this places an approximate upper limit on the ℓ at which the self-calibration can function to a high degree of accuracy. In the future, a more robust bias model could be chosen for the very highly non-linear regime to extend this limit with relative ease, as it will alter only the form of Eq. 27 and the resulting performance calculations, while the method of extracting B_{iii}^{Igg} remains unchanged.

4.5 Other sources of uncertainty

The GGI self-calibration requires the calculation of W_{ijk} and Q_3 , which include the cosmology-dependent lensing kernel. This introduces an uncertainty due to the measurement of Ω_m and the distance-redshift relation. However, we expect this uncertainty to be negligible when compared to other dominant sources of error in the GGI self-calibration. Komatsu et al. (2011) have measured Ω_m to 5% accuracy, and new measurements are expected to constrain Ω_m to 1-2%. The distance-redshift

relation will also be constrained to 1% by baryon acoustic oscillations and supernovae (Albrecht et al. 2006). We expect that given these constraints, any uncertainty introduced by the lensing kernel will only affect the GGI self-calibration at the percent level, which is negligible compared to the expected systematic error δf_{ijk} of Eq. 51. An iterative approach can also be applied, where a set of initial cosmological parameters is chosen as above and used for the 2- and 3-point self-calibration, from which new (improved) parameter constraints can be calculated and applied again until the interactive process converges.

Similarly, we have used an approximate fitting formula derived from perturbation theory by Scoccimarro & Couchman (2001) for the bispectrum in our error estimations. This is only expected to be accurate to within 15% when compared to N-body simulations for the lensing bispectrum. We thus expect uncertainty due to the calculation of the bispectrum to be dominant when compared to errors associated with the power spectrum calculation. A more accurate approach to modelling the bispectrum and the effects of intrinsic alignment will provide more accurate estimates of the GGI self-calibration performance, which we leave to a later work.

Catastrophic photo-z error also affects the GGI self-calibration through the assumed galaxy distribution. We assume a Gaussian photo-z PDF in our numerical calculations, but observed photo-z PDFs generally have non-negligible outliers. This affects the GGI self-calibration through the calculation of Q_3 and the relationship between B^{IGG} and B^{Igg} . However, these effects are suppressed due to both numerator and denominator being affected in similar ways. The effect can be further decreased by better photo-z PDF template estimates and better calibration of photo-z errors, and we expect the GGI self-calibration to ultimately be safe from non-negligible degradation due to catastrophic photo-z errors.

The relationship between B^{IGG} and B^{Igg} depends upon our assumption of a deterministic galaxy bias, which is not perfectly accurate in real galaxy distributions. This could cause both random and systematic error in the GGI self-calibration. A true quantification of this effect is beyond the scope of this paper, as the possible correlation between stochasticity and intrinsic alignment is not well understood. However, Baldauf et al. (2010) has shown that it is possible to suppress the galaxy stochasticity to the 1% level in some cases, which allows that the effect of stochasticity in the GGI self-calibration could ultimately be limited to the percent level, which would be safely negligible compared to other sources of error.

4.6 Summary of residual errors

There are three regimes under which the performance of the GGI self-calibration can be summarised. These are defined by the magnitude of the GGI contamination as represented by f_{ijk}^I . The first is where the ggi correlation is too small to detect in $B^{(2)}$, with $f_{ijk}^I \leq f_{ijk}^{thresh}$. If the intrinsic alignment cannot be detected in $B^{(2)}$, the GGI self-calibration is not applicable. This generally means that the GGI contamination is also negligible when compared to ϵ_{ijk}^{min} , the minimum statistical error in the lensing bispectrum, and there is no need to correct for it.

If $f_{ijk}^I > f_{ijk}^{thresh}$, then the GGI contamination to the lensing bispectrum is likely not negligible, and it must be corrected for. The GGI self-calibration is now able to detect and calculate the GGI correlation. In the second regime, where $\Delta f_{ijk}^{thresh} > \epsilon_{ijk}^{sys} f_{ijk}^I$, the statistical error $\Delta f_{ijk}^{(a)}$ induced by measurement error in the estimator \hat{B}_{iii}^{Igg} is dominant. As shown in Fig. 3, this error is generally negligible when compared to ϵ_{ijk}^{min} , and so in this regime, the GGI self-calibration should perform at the statistical limit of the lensing survey.

Finally, where $\Delta f_{ijk}^{thresh} < \epsilon_{ijk}^{sys} f_{ijk}^I$, the systematic error $\delta f_{ijk} = \epsilon_{ijk}^{sys} f_{ijk}^I$ due to the relationship between B^{IGG} and B_{iii}^{Igg} in Eq. 27 is dominant. In the case where $\epsilon_{ijk}^{sys} < \epsilon_{ijk}^{min} / f_{ijk}^I$, ϵ_{ijk}^{min} is still dominant. Otherwise the GGI self-calibration can suppress the GGI contamination by a factor of 5-10 or more for all but a few adjacent redshift bin choices. In this case, other complementary techniques could be employed to further reduce the GGI contamination down to the statistical limit for the lensing survey.

In the 2-point correlations, one such case has been explored by Zhang (2010b), but such studies of the 3-point intrinsic alignment are left to be done. Zhang, Pen & Bernstein (2010) combines the GI self-calibration with a photo-z self-calibration to better protect the GI self-calibration against catastrophic photo-z effects. Both methods are possible because the GI and GGI self-calibration uses primarily those correlations in one redshift bin to estimate the intrinsic alignment, while Zhang (2010b); Zhang, Pen & Bernstein (2010) use those correlations between redshift bins. As first mentioned in Sec. 1, others have also used information between redshift bins to calibrate the intrinsic alignment contamination in the 2- and 3-point correlations (Okumura T., Jing 2009; Kirk, Bridle & Schneider 2010; Joachimi & Schneider 2008, 2009; Shi, Joachimi & Schneider 2010; Joachimi & Bridle 2010). Such techniques for the 3-point intrinsic alignment correlations should eventually complement the GGI self-calibration for improved reductions in the contamination by the intrinsic alignment in the cosmic shear signal, but much work is left to be done.

5 CONCLUSION

The GGG bispectrum has been shown to be strongly contaminated by the 3-point intrinsic alignment correlations. While the III and GII correlations can be neglected by considering only the cross-correlation bispectrum between three different redshift

bins, the GGI correlation remains a contaminant. Zhang (2010a) first proposed the self-calibration technique in order to calculate and remove the 2-point GI contamination from the GG power spectrum. In this work we verify the performance of the GI self-calibration technique, and expand the self-calibration to the 3-point correlations, proposing the GGI self-calibration technique to calculate and remove the GGI correlation from the GGG bispectrum.

We first establish the estimator \hat{B}_{iii}^{Igg} to extract the ggI correlation from the galaxy ellipticity-density-density measurement for a photo-z galaxy sample. We show that this estimator is expected to be generally applicable to weak lensing surveys and reduces to the simple extraction method for spectroscopic galaxy samples at low photo-z error. We then develop a relation between the GGI and ggI bispectra using the linear and non-linear galaxy bias to relate the galaxy density and cosmic shear measurements. This allows us to calculate and remove the GGI correlation from the GGG bispectrum. While this method is in principle applicable to all ℓ and triangle shapes, we do note some modest restrictions in section 4.4 on very elongated triangles due to the effects of non-Gaussianity and at very non-linear scales due to limitations in the understanding of the galaxy bias model used.

We quantify the performance of the GGI self-calibration technique for a typical weak-lensing survey, using anticipated parameters for the LSST as an example case. The residual statistical error due to measurement uncertainty in the estimator \hat{B}_{iii}^{Igg} is shown to be generally negligible when compared to the minimum measurement error in the lensing bispectrum. By considering the systematic error introduced by the relationship between B_{ijk}^{IGG} and B_{iii}^{Igg} , we show that for galaxy triplets with bins which are not adjacent, $|\epsilon_{ijk}| < 0.1$. For these bin choices, the intrinsic alignment contamination can be suppressed by a factor of 10 or greater. In most cases where two or three bins are adjacent, $|\epsilon_{ijk}| < 0.2$, which allows for a suppression in the contamination by a factor of 5. In only a few of the cases where all three bins are adjacent is $|\epsilon_{ijk}| > 0.2$, and even in these cases we expect a suppression in the contamination by a factor of 3 or more. This will potentially allow the GGI self-calibration to reduce the GGI correlation to the statistical limit of the lensing survey, as discussed in Sec. 4.6.

These results are insensitive to the original intrinsic alignment contamination, such that for any $f_{ijk}^{thresh} < f_{ijk}^I < 1$, the GGI self-calibration will reduce the GGI contamination down to survey limits or by a factor of 5-10 or greater, whichever is less, for all but a few adjacent redshift bin triplets. This is only slightly reduced from the GI self-calibration, where for any $f_{ij}^{thresh} < f_{ij}^I < 1$, the GI self-calibration reduces the GI contamination down to survey limits or by a factor of 10 or greater, whichever is less. We thus expect the GGI self-calibration to perform near the level of the GI self-calibration, and together they promise to be an efficient technique to isolate both the 2- and 3-point intrinsic alignment signals from the cosmic shear signal.

ACKNOWLEDGMENTS

We thank E. Komatsu, R. Mandelbaum, and P. Zhang for useful comments. MI acknowledges that this material is based upon work supported in part by National Science Foundation under grant AST-1109667 and NASA under grant NNX09AJ55G, and that part of the calculations for this work have been performed on the Cosmology Computer Cluster funded by the Hoblitzelle Foundation.

APPENDIX A: CALCULATION OF COEFFICIENTS IN ΔB_{iii}^{IGG}

Upon evaluating the sum and taking the Fourier transform of Eq. 43, each of the products of the correlations have a numerical coefficient due to the restrictions on redshift ordering. Many, however, are identical due to symmetries. The calculation of the unique coefficients a - h in Eqs. 45 & 46 are summarised here. The first coefficient is trivial, due to products with no noise correlations or correlations like $\langle \delta_\alpha \kappa_\nu \rangle$, which are themselves orientation dependent. We then calculate for a term like $\langle \delta_\alpha \delta_\lambda \rangle \langle \delta_\beta \delta_\mu \rangle \langle \kappa_\gamma \kappa_\nu \rangle$

$$\frac{N_P^{-6}}{(1-Q_3)^2} \sum_{\alpha\beta\gamma} \sum_{\lambda\mu\nu} (3S_{\alpha\beta\gamma} - Q_3)(3S_{\lambda\mu\nu} - Q_3) \approx 1. \quad (\text{A1})$$

For terms like $\langle \delta_\alpha^N \delta_\lambda^N \rangle \langle \delta_\beta \delta_\mu \rangle \langle \kappa_\gamma \kappa_\nu \rangle \propto \delta_{\alpha\lambda}$, which include one galaxy density noise correlation

$$a \equiv \frac{N_P^{-5}}{(1-Q_3)^2} \sum_{\alpha\beta\gamma} \sum_{\mu\nu} (3S_{\alpha\beta\gamma} - Q_3)(3S_{\alpha\mu\nu} - Q_3) \approx 1 + \frac{1}{5(1-Q_3)^2}. \quad (\text{A2})$$

For terms like $\langle \delta_\alpha \delta_\lambda \rangle \langle \delta_\beta \delta_\mu \rangle \langle \kappa_\gamma^N \kappa_\nu^N \rangle \propto \delta_{\gamma\nu}$, which include one convergence noise correlation

$$b \equiv \frac{N_P^{-5}}{(1-Q_3)^2} \sum_{\alpha\beta\gamma} \sum_{\lambda\mu} (3S_{\alpha\beta\gamma} - Q_3)(3S_{\lambda\mu\gamma} - Q_3) \approx 1 + \frac{4}{5(1-Q_3)^2}. \quad (\text{A3})$$

For terms like $\langle \delta_\alpha^N \delta_\lambda^N \rangle \langle \delta_\beta^N \delta_\mu^N \rangle \langle \kappa_\gamma \kappa_\nu \rangle \propto \delta_{\alpha\lambda} \delta_{\beta\mu}$, which include two galaxy density noise correlations

$$c \equiv \frac{N_P^{-4}}{(1-Q_3)^2} \sum_{\alpha\beta\gamma} \sum_{\nu} (3S_{\alpha\beta\gamma} - Q_3)(3S_{\alpha\beta\gamma} - Q_3) \approx 1 - \frac{1}{4(1-Q_3)^2}. \quad (\text{A4})$$

For terms like $\langle \delta_\alpha^N \delta_\lambda^N \rangle \langle \delta_\beta^N \delta_\mu^N \rangle \langle \kappa_\gamma^N \kappa_\nu^N \rangle \propto \delta_{\alpha\lambda} \delta_{\gamma\nu}$, which include one galaxy density noise correlation and one convergence noise correlation

$$d \equiv \frac{N_P^{-4}}{(1-Q_3)^2} \sum_{\alpha\beta\gamma} \sum_{\mu} (3S_{\alpha\beta\gamma} - Q_3)(3S_{\alpha\mu\gamma} - Q_3) \approx 1 + \frac{5}{4(1-Q_3)^2}. \quad (\text{A5})$$

For terms like $\langle \delta_\alpha^N \delta_\lambda^N \rangle \langle \delta_\beta^N \delta_\mu^N \rangle \langle \kappa_\gamma^N \kappa_\nu^N \rangle \propto \delta_{\alpha\lambda} \delta_{\beta\mu} \delta_{\gamma\nu}$, which include only noise correlations

$$e \equiv \frac{N_P^{-3}}{(1-Q_3)^2} \sum_{\alpha\beta\gamma} (3S_{\alpha\beta\gamma} - Q_3)^2 \approx 1 + \frac{2}{(1-Q_3)^2}. \quad (\text{A6})$$

For terms like $\langle \delta_\alpha \delta_\lambda \rangle \langle \kappa_\gamma \delta_\mu \rangle \langle \kappa_\nu \delta_\beta \rangle$, which include two correlations with the orientation dependence described in Eq. 44

$$\begin{aligned} f &\equiv \frac{N_P^{-6}}{(1-Q_3)^2} \sum_{\alpha\beta\gamma} \sum_{\lambda\mu\nu} (3S_{\alpha\beta\gamma} - Q_3)(3S_{\lambda\mu\nu} - Q_3) \frac{1}{2} \left(\frac{S_{\mu\gamma}}{(1-Q_2)} + \frac{S_{\gamma\mu}}{Q_2} \right) \frac{1}{2} \left(\frac{S_{\beta\nu}}{(1-Q_2)} + \frac{S_{\nu\beta}}{Q_2} \right) \\ &\approx \frac{5Q_3^2 - Q_3(3 + 13Q_2 + 2Q_2^2) + 5Q_2(1 + 2Q_2)}{80Q_2^2(1-Q_2)^2(1-Q_3)^2}. \end{aligned} \quad (\text{A7})$$

For terms like $\langle \delta_\alpha^N \delta_\lambda^N \rangle \langle \kappa_\gamma \delta_\mu \rangle \langle \kappa_\nu \delta_\beta \rangle \propto \delta_{\alpha\lambda}$, which include two correlations with the orientation dependence described in Eq. 44 and one galaxy density noise correlation

$$\begin{aligned} g &\equiv \frac{N_P^{-5}}{(1-Q_3)^2} \sum_{\alpha\beta\gamma} \sum_{\mu\nu} (3S_{\alpha\beta\gamma} - Q_3)(3S_{\alpha\mu\nu} - Q_3) \frac{1}{2} \left(\frac{S_{\mu\gamma}}{(1-Q_2)} + \frac{S_{\gamma\mu}}{Q_2} \right) \frac{1}{2} \left(\frac{S_{\beta\nu}}{(1-Q_2)} + \frac{S_{\nu\beta}}{Q_2} \right) \\ &\approx \frac{3 + 5Q_3^2 - Q_3(3 + 13Q_2 + 2Q_2^2) + 15Q_2^2}{80Q_2^2(1-Q_2)^2(1-Q_3)^2}. \end{aligned} \quad (\text{A8})$$

Finally, for terms like $\langle \delta_\alpha^N \delta_\lambda^N \rangle \langle \kappa_\gamma \delta_\mu \rangle \langle I_\nu \delta_\beta \rangle \propto \delta_{\alpha\lambda}$, which include one correlation with the orientation dependence described in Eq. 44 and one galaxy density noise correlation

$$\begin{aligned} h &\equiv \frac{N_P^{-5}}{(1-Q_3)^2} \sum_{\alpha\beta\gamma} \sum_{\mu\nu} (3S_{\alpha\beta\gamma} - Q_3)(3S_{\alpha\mu\nu} - Q_3) \frac{1}{2} \left(\frac{S_{\mu\gamma}}{(1-Q_2)} + \frac{S_{\gamma\mu}}{Q_2} \right) \\ &\approx \frac{20Q_3^2 - 5Q_3(5 + 6Q_2) + 6(1 + 6Q_2)}{80Q_2(1-Q_2)(1-Q_3)^2}. \end{aligned} \quad (\text{A9})$$

For typical values $Q_2 = 1/2$ and $Q_3 = 2/5$, these coefficients are

$$\begin{aligned} a &= \frac{14}{9} \approx 1.6 \\ b &= \frac{29}{9} \approx 3.2 \\ c &= \frac{11}{36} \approx 0.3 \\ d &= \frac{161}{36} \approx 4.5 \\ e &= \frac{59}{9} \approx 6.6 \\ f &= 1 \\ g &= \frac{71}{36} \approx 2.0 \\ h &= \frac{14}{9} \approx 1.5. \end{aligned} \quad (\text{A10})$$

REFERENCES

- Acquaviva V., Hajian A., Spergel D., Das S., 2008, PRD, 78, 043514
- Albrecht A., et al., 2006, Report of the Dark Energy Task Force, arXiv:astro-ph/0609591
- Bacon D.J., Refregier A.R., Ellis R.S., 2000, MNRAS, 318, 625
- Bacon D.J., Refregier A., Clowe D., Ellis R.S., 2001, MNRAS, 325, 1065
- Baldauf T., Smith R., Seljak U., Mandelbaum R., 2010, PRD, 81, 063531
- Bean R., Tangmatitham M., 2010, PRD, 81, 083534
- Bernstein G.M., 2009, ApJ, 695, 652
- Bernstein G.M., Jarvis M., 2002, AJ, 123, 583
- Blazek J., McQuinn M., Seljak U., 2011, JCAP, 05, 010
- Bridle S., King L., 2007, New J. Phys. 9, 444
- Brown M.L., Taylor A.N., Hambly N.C., Dye S., 2002, MNRAS, 333, 501
- Brown M.L., Taylor A.N., Bacon D.J., Gray M.E., Dye S., Meisenheimer K., Wolf C., 2003, MNRAS, 341, 100
- Capozziello S., Cardone V.F., Troisi A., 2006, PRD, 73, 104019
- Catelan P., Kamionkowski M., Blandford R.D., 2001, MNRAS, 320, L7
- Cooray A., Sheth R., 2002, Phys. Rept. 372, 1
- Crittenden R.G., Natarajan P., Pen U.-L., Theuns T., 2001, ApJ, 559, 552
- Croft R., Metzler C., 2000, ApJ, 545, 561
- Daniel S., Caldwell R., Cooray A., Melchiorri A., 2008, PRD, 77, 103513
- Daniel S., Linder E., Smith T., Caldwell R., Corray A., Leauthaud A., Lombriser L., 2010, PRD, 80, 123508
- Dossett J., Moldenhauer J., Ishak M., 2011, PRD, 84, 023012
- Eisenstein D.J., Hu W., Tegmark M., 1999, ApJ, 518, 2
- Erben T., Van Waerbeke L., Bertin E., Mellier Y., Schneider P., 2001, A&A, 366, 717
- Faltenbacher A., Li C., White S.D.M., Jing Y.P., Mao S., Wang J., 2009, Res. Astron. & Astrophys., 9, 41
- Fry J., 1994, PRL, 73, 215
- Fry J.N., Gaztanaga E., 1993, ApJ, 413, 447
- Fu X., Wu P., Yu H., 2009, PLB, 677, 12
- Heavens A., Refregier A., Heymans C., 2000, MNRAS, 319, 649
- Heymans C., Heavens A., 2003, MNRAS, 339, 711
- Heymans C., Brown M., Heavens A., Meisenheimer K., Taylor A., Wolf C., 2004, MNRAS, 347, 895
- Heymans C., White M., Heavens A., Vale C., Van Waerbeke L., 2006, MNRAS, 371, 750
- Hirata C.M., Seljak U., 2003, MNRAS, 343, 459
- Hirata C.M., Seljak U., 2003, PRD, 67, 43001
- Hirata C.M., Seljak U., 2004, PRD, 70, 063526
- Hirata C.M., Mandelbaum R., Ishak M., Seljak U., Nichol R., Pimblet K.A., Ross N.P., Wake D., 2007, MNRAS, 381, 1197
- Hoekstra H., Yee H.K.C., Gladders M.D., Barrientos L.F., Hall P.B., Infante L., 2002, ApJ, 72, 55
- Hu W., 2002, PRD, 65, 023003
- Hu W., Tegmark M., 1999, ApJL, 514, L65
- Huterer D., Linder E., 2007, PRD, 75, 023519
- Ishak M., Dossett J., 2009, PRD, 80, 043004
- Ishak M., Hirata C.M., McDonald P., Seljak U., 2004, PRD, 69, 083514
- Ishak M., Upadhye A., Spergel D., 2006, PRD, 74, 043513
- Jarvis M., Bernstein G.M., Fischer P., Smith D., Jain B., Tyson J.A., Wittman D., 2003, AJ, 125, 1014
- Jing Y.P., 2002, MNRAS, 335, 89
- Jeong D., Komatsu E., 2009, ApJ, 703, 1230
- Joachimi B., Bridle S., 2010, A&A, 523, A1
- Joachimi B., Schneider P., 2008, A&A, 488, 829
- Joachimi B., Schneider P., 2009, A&A, 507, 105
- Joachimi B., Schneider P., 2010, A&A, 517, A4
- Joachimi B., Mandelbaum R., Abdalla F., Bridle S., 2010, A&A, 527, A26
- Joudaki S., Cooray A., Holz D.E., 2009, PRD, 80, 023003,
- King L., 2005, A&A, 441, 47
- King L., Schneider P., 2002, A&A, 396, 411
- King L., Schneider P., 2003, A&A, 398, 23
- Kirk D., Bridle S., Schneider M., 2010, MNRAS, 408, 1502
- Komatsu E., et al., 2011, ApJS, 192, 18

- Krause E., Hirata C.M., 2011, MNRAS, 410, 2730
Linder E., Cahn R., 2007, *Astropart. Phys.* 28, 481
LSST Science Collaborations and LSST Project, 2009, LSST Science Book, Version 2.0, arXiv:astro-ph/0912.0201, <http://www.lsst.org/lsst/scibook/>
Mandelbaum R., Hirata C.M., Ishak M., Seljak U., Brinkmann J., 2006, MNRAS, 367, 611
Massey R., Refregier A., Bacon D., Ellis R., 2005, MNRAS, 359, 1277
Okumura T., Jing Y.P., 2009, *ApJL*, 694, L83
Pen U.-L., Lu T., Van Waerbeke L., Mellier Y., 2003, MNRAS, 346, 994
Refregier A., 2003, *Ann. Rev. A&A*, 41, 645
Rhodes J., Refregier A., Groth E.J., 2001, *ApJL*, 552, L85
Schmidt F., 2008, *PRD*, 78, 043002
Schrabback T. et al., 2010, *A&A*, 516, A63
Soccimarro R., Couchman H., 2001, MNRAS, 325, 1312
Semboloni E., Heymans C., Van Waerbeke L., Schneider P., 2008, MNRAS, 388, 991
Semboloni E., Schrabback T., Van Waerbeke L., Vafaei S., Hartlap J., Hilbert S., 2010, MNRAS, 410, 143
Simpson F., James J., Heavens A., Heymans C., 2011, arXiv:astro-ph/1107.5169
Shi X., Joachimi B., Schneider P., 2010, *A&A*, 523, A60
Song Y.S., 2005, *PRD*, 71, 024026
Takada M., Jain B., 2003, MNRAS, 340, 580
Takada B., Jain M., 2004, MNRAS, 348, 897
Takada M., White M., 2004, *ApJL*, 601, L1
Thomas S., Abdalla F., Weller J., 2009, MNRAS, 395, 197
Toreno I., Semboloni E., Schrabback T., 2010, *A&A*, 530, A68
Vafaei S., Lu T., Van Waerbeke L., Semboloni E., Heymans C., Pen U.-L., 2010, *Astropart. Phys.* 32, 340
Van Waerbeke L., Mellier Y., 2003, *ArXiv Astrophysics e-prints*, astro-ph/0305089
Van Waerbeke L. et al., 2000, *A&A*, 358, 30
Van Waerbeke L., Mellier Y., Pell R., Pen U.-L., McCracken H.J., Jain B., 2002, *A&A*, 393, 369
Zaldarriaga M., Spergel D.N., Seljak U., 1997, *ApJ*, 488, 1
Zhang P., 2010, *ApJ*, 720, 1090
Zhang P., 2010, MNRAS, 406, L95
Zhang P.J., Liguori M., Bean R., Dodelson S., 2007, *PRL*, 99, 141302
Zhang P., Pen U.-L., Bernstein G., 2010, MNRAS, 405, 359
Zhao H., Bacon D.J., Taylor A.N., Horne K., 2006, MNRAS, 368, 171
Zhao G., Pogosian L., Silvestri A., Zylberberg J., 2009, *PRD*, 79, 083513